General Disclaimer

One or more of the Following Statements may affect this Document

- This document has been reproduced from the best copy furnished by the organizational source. It is being released in the interest of making available as much information as possible.

- This document may contain data, which exceeds the sheet parameters. It was furnished in this condition by the organizational source and is the best copy available.

- This document may contain tone-on-tone or color graphs, charts and/or pictures, which have been reproduced in black and white.

- This document is paginated as submitted by the original source.

- Portions of this document are not fully legible due to the historical nature of some of the material. However, it is the best reproduction available from the original submission.

SQT

REPORT ON

MATHEMATICAL MODEL FOR ISOELECTRIC FOCUSING: COMPUTER SIMULATION AND IMPLEMENTATION

PREPARED FOR

MR. J. A. VITALE
OFFICE OF UNIVERSITY AFFAIRS
NATIONAL AERONAUTICS AND SPACE ADMINISTRATION
WASHINGTON, D.C. 20546

BY

BIOPHYSICS TECHNOLOGY LABORATORY
UNIVERSITY OF ARIZONA, TUCSON, AZ. 85721

NASA GRANT NSG-7333
FEBRUARY 5, 1979

(NASA-CR-158128) MATHEMATICAL MODEL FOR STEADY STATE, SIMPLE AMPHOLYTE ISOELECTRIC FOCUSING: DEVELOPMENT, COMPUTER SIMULATION AND IMPLEMENTATION (Arizona Univ., Tucson.) 80 p HC A05/MF A01 CSCL 07C G3/23

N79-17905

Unclas
16301

SIGILLVM VNIVERSITATIS ARIZONENSIS
ESTABLISHED 1885

ENGINEERING EXPERIMENT STATION
COLLEGE OF ENGINEERING
THE UNIVERSITY OF ARIZONA
TUCSON, ARIZONA

TABLE OF CONTENTS

1. DEVELOPMENT OF A MATHEMATICAL MODEL FOR STEADY STATE ISOELECTRIC FOCUSING.

Isoelectric focusing (IEF) is a high resolution electrophoretic technique which is widely employed for protein separations. The technique is based upon the observation that proteins exhibit zero mobility at unique positions (their isoelectric points) in a pH gradient. The introduction by LKB (under the tradename Ampholine) of mixtures of synthetically random polyaminopolycarboxylic acids provided an easy means of establishing a broad pH gradient and contributed to a large extent to the remarkable popularity of the analytical technique. Preparative IEF has enjoyed less popularity as a result of (a) scaling constraints of the classical focusing apparatus, (b) the loss during fractionation of the resolution achieved during focusing, and (c) the unavoidable contamination by Ampholine of the fractionated proteins. We are addressing the last of these problems and proposing the elimination of Ampholine from the system by establishing the pH gradient with simple ampholytes. To that end we have developed a mathematical model of simple ampholyte IEF. A simple ampholyte in our terminology is one whose behavior near its isoelectric point results from the influence of only two ionizeable groups. Predictions of the model and computer simulation of focusing experiments are of direct importance to our efforts to obtain Ampholine-free, stable pH gradients.

1.1. Simple Model based on the Electroneutrality Approximation.

Our first effort to develop a model of IEF was largely directed by Svensson's pioneering work[1] in the early 1960's. He considered the focusing of a single ampholyte component, and we generalized the treatment to two, three and multi-component systems. This

[1] H. Svensson, Acta Chem. Scand. 15, 325-341 (1961)

approach employs the common form of Ohm's law to describe the electric field as a function of the solution conductance. The model consists of an ordinary differential equation for each ampholyte which is a statement of conservation of mass, and a coupling algebraic equation which represents the electroneutrality approximation. The model equations were solved using discretization techniques based on the Runge-Kutta-Merson integration rule and the solution was implemented on a digital computer using DARE P simulation software[2]. The results of the solution were presented as the pH, conductance, and the concentration of each ampholyte as a function of distance along the column axis. This model was used for the computer simulations discussed later in this report. The salient aspects of the model are described in a paper, "Theory and Computer Simulation of Isoelectric Focusing with Simple Ampholytes", submitted to the LKB Symposium - Electrofocus 78 and included in Appendix A. The developemnt of the multi-component system is included as Appendix B.

As a result of comments from Dr. Dudley Saville during a visit to our laboratory and subsequent communications[3], we have reappraised this model. Dr. Saville indicated that the contribution of the current due to diffusion should be considered in calculating the effective electric field, i.e., a more complete expression of Ohm's law must be employed for a rigorous treatment. The effect of this correction will of course be dependent upon the magnitude of the diffusion current relative to the applied current. Our preliminary calculations indicate that this is not large for the cases considered; however, we feel it is necessary to specifically include the diffusion current in the

[2]J. J. Lucas and J. V. Wait, DARE P - A Portable CSSL-Type Simulation Language, Simulation (1975)

[3]D. A. Saville, personal communication

general form of the model and neglect its contribution only when it can be shown to be negligible.

1.2. Revised General Model of Steady State Isoelectric Focusing.

The revised model describing a one-dimensional IEF system is based upon the following assumptions:

(1) the system is at steady state, i.e. there is no net flux of any ampholyte component;

(2) the concentrations of component subspecies are described by equations of chemical equilibria, i.e. chemical reactions (proton associations and dissociations) are rapid relative to transport processes;

(3) the system is isothermal and there is no macroscopic flow.

1.2.1. General Equations.

Flux (F_i) of i-th species

$$-F_i = e\, w_i z_i n_i \nabla\phi + RT\, w_i \nabla n_i \qquad (1)$$

w_i - mobility ($m^2 sec^{-1} V^{-1}$)

n_i - concentration ($moles/m^3$)

z_i - valence (dimensionless)

ϕ - local electric potential (V)

R - universal gas constant (8.314 joules/^oK . mole)

e - molar charge ($6.9366.10^4$ Q)

T - temperature (^oK)

Q - Coulomb's unit change

Conservation of mass (conservation of i-th ions)

$$\nabla \cdot F_i + R_i = 0 \qquad (2)$$

R_i - rate of production of i-th species per unit volume (rate of change of charge density) ($\frac{Q}{m^3\ sec}$)

Poisson's equation

$$\varepsilon \nabla^2 \phi = -e \sum_{i=1}^{N} z_i n_i \qquad (3)$$

ε - dielectric constant ($5.48 \cdot 10^{-11}\ \frac{Q}{V.m}$)

N - number of species

Conservation of charge (net production of charge is zero)

$$\sum_{1}^{N} z_i R_i = 0 \qquad (4)$$

Conservation of j-th ampholyte

$$\sum_{i=j_1}^{i=j_2} R_i = 0 \qquad (5)$$

$R_{j_1}, R_{j_1+1}, \ldots, R_{j_2}$ - rate of production

of species $(j_1, j_1+1, \ldots, j_2)$ - component subspecies

of j-th ampholyte

1.2.2. Model Construction.

The conservation of charge equation: Multiplying equation (2) by the valence z_i and adding these equations for all species gives

$$\sum_{i=1}^{N} z_i \nabla . F_i + \sum_{i=1}^{N} z_i R_i = 0 \qquad (6)$$

Taking into account (4) the above equation becomes

$$\sum_{i=1}^{N} z_i \nabla . F_i = 0 \qquad (7)$$

or

$$\nabla . \sum_{i=1}^{N} z_i F_i = 0 \qquad (8)$$

Since valences z_i are constant.

From here we will treat only the one dimensional case, when the symbol ∇ represents the derivative, that means we substitute $\nabla = \frac{d}{dx}$.

Equation (8) can be integrated once, giving

$$\sum_{i=1}^{N} z_i F_i = -J$$

J - total current density

Using (1) in the above we get

$$e\left(\sum_{i=1}^{N} z_i^2 w_i n_i\right) \frac{d\phi}{dx} + RT \sum_{i=1}^{N} z_i w_i \frac{dn_i}{dx} = -J \qquad (9)$$

Ampholyte conservation: A procedure similar to one used in above can be applied here. The equations (2) for component subspecies of j-th ampholyte are added, which results in

$$\sum_{i=j_1}^{i=j_2} \frac{dF_i}{dx} + \sum_{i=j_1}^{i=j_2} R_i = 0 \qquad (10)$$

Using (5) in the above equation leads to the following relation

$$\frac{d}{dx} \sum_{i=j_1}^{i=j_2} F_i = 0 \qquad (11)$$

The equation (10) can be integrated, which results in

$$\sum_{i=j_1}^{i=j_2} F_i = c_j \qquad (12)$$

$$j = 1,2,\ldots,M$$

M - number of ampholytes

The flux of any ampholyte is zero

$$c_j = 0 \qquad (13)$$

since we assume steady state.

This results in the following M equations

$$\sum_{i=j_1}^{i=j_2} F_i = 0 \qquad (14)$$

Using (1) in (14) gives

$$e\left(\sum_{i=j_1}^{i=j_2} z_i w_i n_i\right) \frac{d\phi}{dx} + RT \sum_{i=j_1}^{i=j_2} w_i \frac{dn_i}{dx} = 0 \qquad (15)$$

The equation (9) and equations (14) constitute a system of M+1 equations with N unknowns $(n_1, n_2, \ldots, n_N)$. For model completeness, some other relations are needed since N > M+1.

Chemical Equilibria:

We assume that the chemical equilibria are obtained rapidly with respect to transport processes, and that the concentrations of component subspecies are related by the dissociation constants. To illustrate this approach let us consider an ampholyte A_j which dissociates into simple valence ions i.e. A_j^+ and A_j^- .

We use the following notation

Species: H^+ OH^- .... A_j A_j^+ A_j^-

Concentrations: n_1 n_2 ..... n_{j_1} n_{j_1+1} n_{j_2}

$$A_j^- + H^+ \underset{c_2}{\overset{c_1}{\rightleftharpoons}} A_j \quad ; \qquad K_{j_1} = \frac{c_4}{c_3}$$

$$A_j + H^+ \underset{c_4}{\overset{c_3}{\rightleftharpoons}} A_j^+ \quad ; \qquad K_{j_2} = \frac{c_2}{c_1}$$

The dissociation constants are

$$K_{j_1} = \frac{n_1 n_{j_1}}{n_{j_1+1}}$$

$$K_{j_2} = \frac{n_1 n_{j_2}}{n_{j_1}} \qquad (16)$$

$$K_w = n_1 n_2$$

It is possible to use (16) in order to express n_{j_1+1}, n_{j_2} and n_2 in terms of n_1 and n_{j_1}, thus reducing the number of variables in the model. We can proceed similarly in the cases of more complex ampholytes, which dissociating lead to more then 3 component subspecies. This

way we can express the concentrations of component subspecies of an ampholyte in terms of the hydrogen ion concentration (n_1) and either the concentration of one chosen component subspecies or the total ampholyte concentration (n_{t_j})

$$n_{t_j} = \sum_{i=j_1}^{i=j_2} n_i \qquad (17)$$

1.2.3. Isoelectric Focusing Model With a Single Simple Ampholyte Example.

Notation

i:	1	2	3	4	5
Species:	H^+	OH^-	A	A^+	A^-
Concentration:	n_1	n_2	n_3	n_4	n_5

$$H_2O \underset{c_2}{\overset{c_1}{\rightleftharpoons}} H^+ + OH^- \qquad K_w = n_1 n_2$$

$$A^- + H^+ \underset{c_4}{\overset{c_3}{\rightleftharpoons}} A \qquad K_2 = \frac{c_4}{c_3}$$

$$A + H^+ \underset{c_6}{\overset{c_5}{\rightleftharpoons}} A^+ \qquad K_1 = \frac{c_6}{c_5}$$

$$K_1 = \frac{n_1 n_3}{n_4} \qquad (18)$$

$$K_2 = \frac{n_1 n_5}{n_3}$$

$$K_w = n_1 n_2 \qquad (19)$$

$z_1 = 1,\ z_2 = -1,\ z_3 = 0,\ z_4 = 1,\ z_5 = -1$

For this example we have only one ampholyte (M=1) and $j_1 = 3$, $j_2 = 5$.

From the equation (9) we obtain

$$e\left(\sum_1^5 z_i^2 w_i n_i\right) \frac{d\phi}{dx} + RT \sum_1^5 z_i w_i \frac{dn_1}{dx} = -J \qquad (20)$$

Similarly from (15) we have

$$e\left(\sum_{3}^{5} z_i w_i n_i\right) \frac{d\phi}{dx} + RT \sum_{3}^{5} w_i \frac{dn_1}{dx} = 0 \qquad (21)$$

Using (18) and (19) we can write

$$n_2 = \frac{K_w}{n_1}$$

$$n_5 = \frac{n_3 K_2}{n_1} \qquad (22)$$

$$n_4 = \frac{n_1 n_3}{K_1}$$

From (22) we compute

$$\frac{dn_2}{dx} = -\frac{K_w}{n_1^2} \frac{dn_1}{dx}$$

$$\frac{dn_4}{dx} = \frac{n_3}{K_1} \frac{dn_1}{dx} + \frac{n_1}{K_1} \frac{dn_3}{dx} \qquad (23)$$

$$\frac{dn_5}{dx} = -\frac{K_2}{n_1^2} n_3 \frac{dn_1}{dx} + \frac{K_2}{n_1} \frac{dn_3}{dx}$$

Using (22) and (23) in (20) we obtain after some simple manipulations

$$\left(w_1 + w_2 \frac{K_w}{n_1^2} + w_4 \frac{n_3}{K_1} + w_5 \frac{K_2 n_3}{n_1^2}\right) \frac{dn_1}{dx} + \left(\frac{w_4}{K_1} n_1 - w_5 \frac{K_2}{n_1}\right) \frac{dn_3}{dx} =$$

$$= \frac{-J}{RT} - \frac{e}{RT} \left(w_1 n_1 + w_2 \frac{K_w}{n_1} + w_4 \frac{n_1 n_3}{K_1} + w_5 \frac{n_3 K_2}{n_1}\right) \frac{d\phi}{dx} \qquad (24)$$

Similarly using (22) and (23) in (21) we obtain

$$\left(\frac{w_4}{K_1} n_3 - w_5 K_2 \frac{n_3}{n_1^2}\right) \frac{dn_1}{dx} + \left(w_3 + \frac{w_4}{K_1} n_1 + w_5 \frac{K_2}{n_1}\right) \frac{dn_3}{dx} =$$

$$= - \frac{e}{RT} \left(w_4 \frac{n_1 n_3}{K_1} - w_5 K_2 \frac{n_3}{n_1} \right) \frac{d\phi}{dx} \qquad (25)$$

Equation 3 becomes

$$(-\varepsilon/e) \frac{d^2\phi}{dx^2} = n_1 - n_2 + n_4 - n_5 \qquad (26)$$

Taking into account the value[4] of the constant ($\varepsilon/e = 6.06 \times 10^{-16}$) and assuming the rate of change of the electric field is much smaller than 10^{15} V m^{-2}, we replace Poisson's equation by an algebraic one, representing the electroneutrality approximation. Using (22) we write

$$n_1 - K_w \frac{1}{n_1} + \frac{1}{K_1} n_1 n_3 - K_2 (n_3/n_1) = 0 \qquad (27)$$

1.3. Direction of Continuing Research.

We have a mathematical model of steady state IEF based on the electroneutrality approximation which has been written in the forms for single and multicomponent systems. We have a revised general mathematical model of steady state IEF, which has been written for the single ampholyte system. We intend to solve the equations for the single component system in both forms and compare their solutions and results. Using the most advantageous approach, we will then address multiple component focusing systems. No major difficulties are forseen at the level of two and three components. At this level we will attempt quantitative experimental verification of the model and conduct remodeling if required. The feasibility of achieving a solution with several ampholyte components will be evaluated and implemented if considered reasonable. We intend to express the

[4] S. R. Vaccaro and H. S. Green, Ionic Processes in Excitable Cells (manuscript)

equations in terms of the total concentration of each ampholyte.

We also intend to evaluate the feasibility of extending the model to consider the transient state. A transient state solution would, in addition to enlarging the theoretical foundation of isoelectric focusing, provide additional insight into the mechanics of the approach to steady state. This may allow further exploitation of the process as a kinetic rather than static event, and lead to increases in time efficiency. This last factor may be quite important as the time required for focusing the gradient can be considerable. Dr. D. Saville will be providing us with collaborative assistance during the coming year.

2. COMPUTER SIMULATIONS OF STEADY STATE IEF

2.1. Simulations and Their Evaluation.

Computer simulations are intended to serve three functions in our research. First, the simulations increase our understanding of the focusing process by allowing us to vary ampholyte characteristics or experimental conditions and observe their affect on the IEF system. Second, the simulations provide theoretical data against which the experimental data may be compared to establish the validity of the theoretical model and its parameters. Third, the method of simulation will hopefully be developed to the level that it may provide the basis for designing focusing systems with specifically desired characteristics.

Computer simulations have been conducted with a variety of ampholyte systems at the level of two and three components using the simple model. The simulations are set up by entering specific values for the applied current, the initial (boundary) concentrations of the ampholytes, and the

physicochemical characteristics for each ampholyte which define its electrophoretic behavior, i.e., its proton dissociation constants, mobility, and diffusion constant. In some cases these parameters have been given values which reflect a real compound, while in other cases values representing purely imaginary components have been used. The latter method allows sequential variation of a given paramenter (or set) to establish what effect this variation will have on the characteristics of the focusing system. The index of the library of computer simulations we have conducted is included as Appendix C. For the comparison of related systems, the boundary concentrations of each component may be established as different (to represent a limit of the column) or as equal (to represent some intermediate position). When using equal concentrations of both components as the boundary condition in a two component system, the simulation may be directed toward either the anode or the cathode. To represent a given experimental setup, the cross-sectional area of the column and its length must be specified to allow integration of the ampholyte concentrations over these dimensions. The integrated values are then the total amount of ampholyte contained within the column volume. The simulations have routinely been conducted using the dimensions of the ISCO Column Model 212 which is one of the focusing apparatus routinely employed in our laboratory.

The results of a simulation using two components representing glutamic acid and histidine are illustrated by the concentration profiles (figure 1) and the conductivity and pH profiles (figure 2). The conductivity and pH profiles are of course of primary interest in regard to utilization of the focusing system, while the concentration profiles are of interest in that they represent the manner in which the

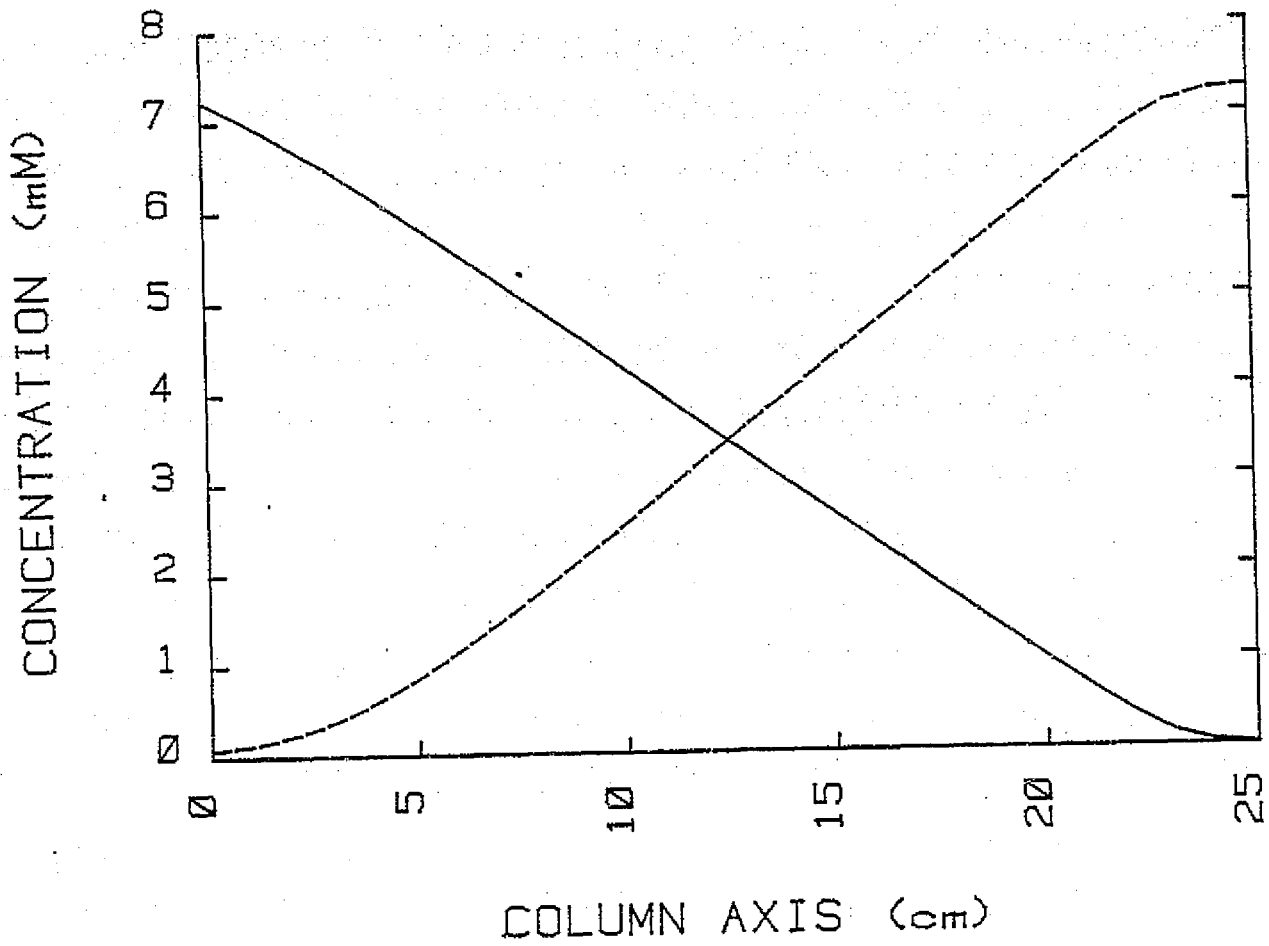

Fig. 1: The concentration profiles of the two-component IEF system using glutamic acid (solid line) and histidine (broken line). The current employed was 4 x 10^{-7}A.

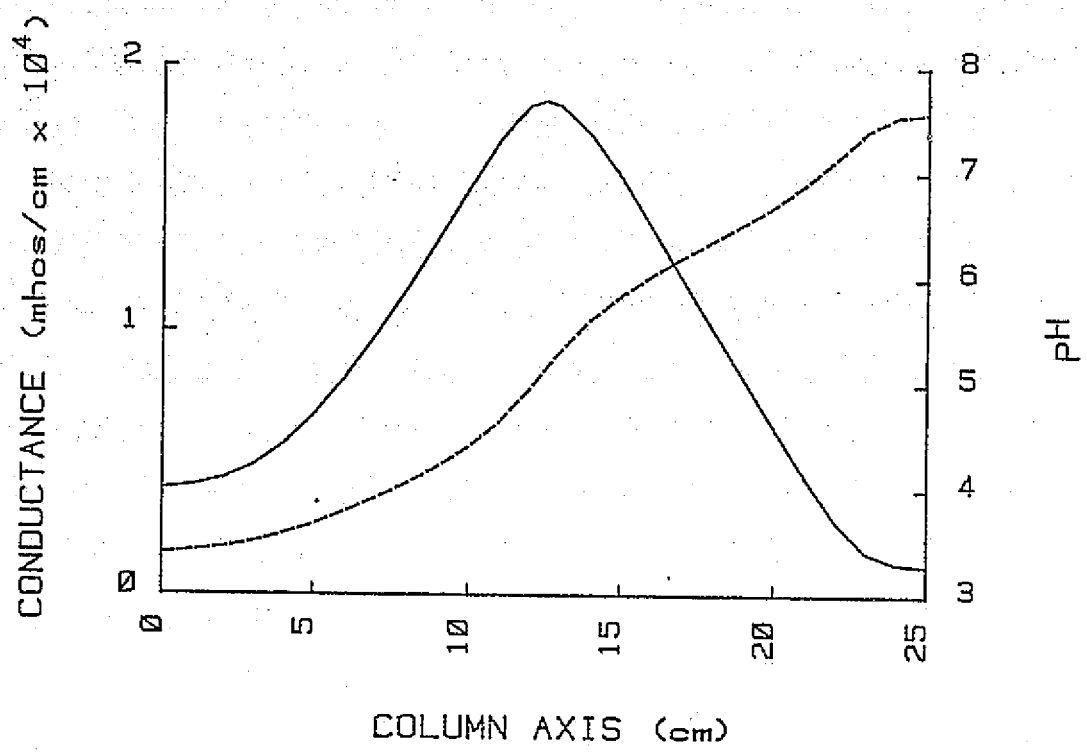

Fig. 2: The conductivity (solid line) and pH (broken line) profiles of the two-component IEF system. The conditions were identical to Fig. 1.

pH and conductivity are established. The profiles obtained from a series of simulations may be replotted together to demonstrate the effect of parameter variation. The pH and conductivity data presented in figures 3 and 4 were generated by setting the pK's of one ampholyte (pK_{B1}= 6 and pK_{B2}= 8) while varying the pK's of the other ampholyte systematically so that the Δ pK, i.e. $pK_{A2} - pK_{A1}$, is held constant while the pI of the component varies. The boundary width, e.g. roughly the distance between points representing 5% and 95% of one of the components maximum concentration, reflected in these profiles decreases at large values of $pI_B - pI_A$ and increases for small values of this parameter. The pH data in figure 5 were generated by holding the pK's of one ampholyte constant and varying the $pK_{A2} - pK_{A1}$ value of the other without changing its pI. The boundary represented by these profiles sharpens at small values of $pK_2 - pK_1$ for either ampholyte and broadens for large values of this parameter. These figures also indicate that rather linear, shallow pH gradients may be established with ampholytes having either a small Δ pK (good ampholytes) or a large Δ pK (poor ampholytes). The pH and conductivity data of figures 6 and 7 respectively were generated varying the equal boundary concentrations of both components. In this case the parameters were specified to represent one poor ampholyte (Δ pK = 6, pI = 5) and one good ampholyte (Δ pK = 2, pI = 7). It can be seen that the higher concentrations produced more linear pH profiles over a narrow range and higher conductivity with a concomitant reduction in boundary sharpness.

It was noted that the width of the boundary between two ampholyte components is inversely proportional to the amperage. The effect of

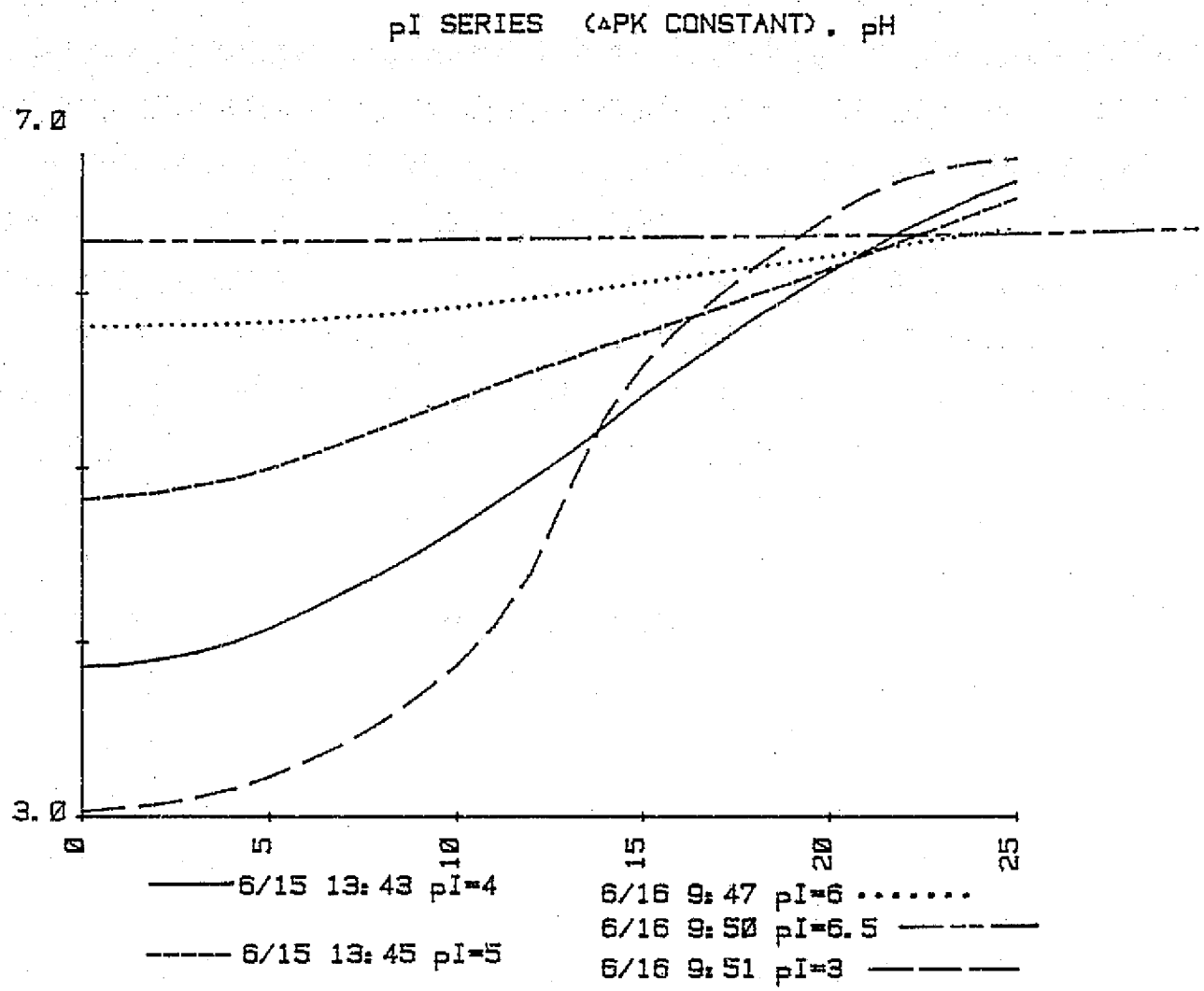

Fig. 3: The pH profiles generated using one component with a pI of 7, while the pK's of the other component were varied so that the pI ranged from 3 to 6.5. The current employed was 4×10^{-7}A.

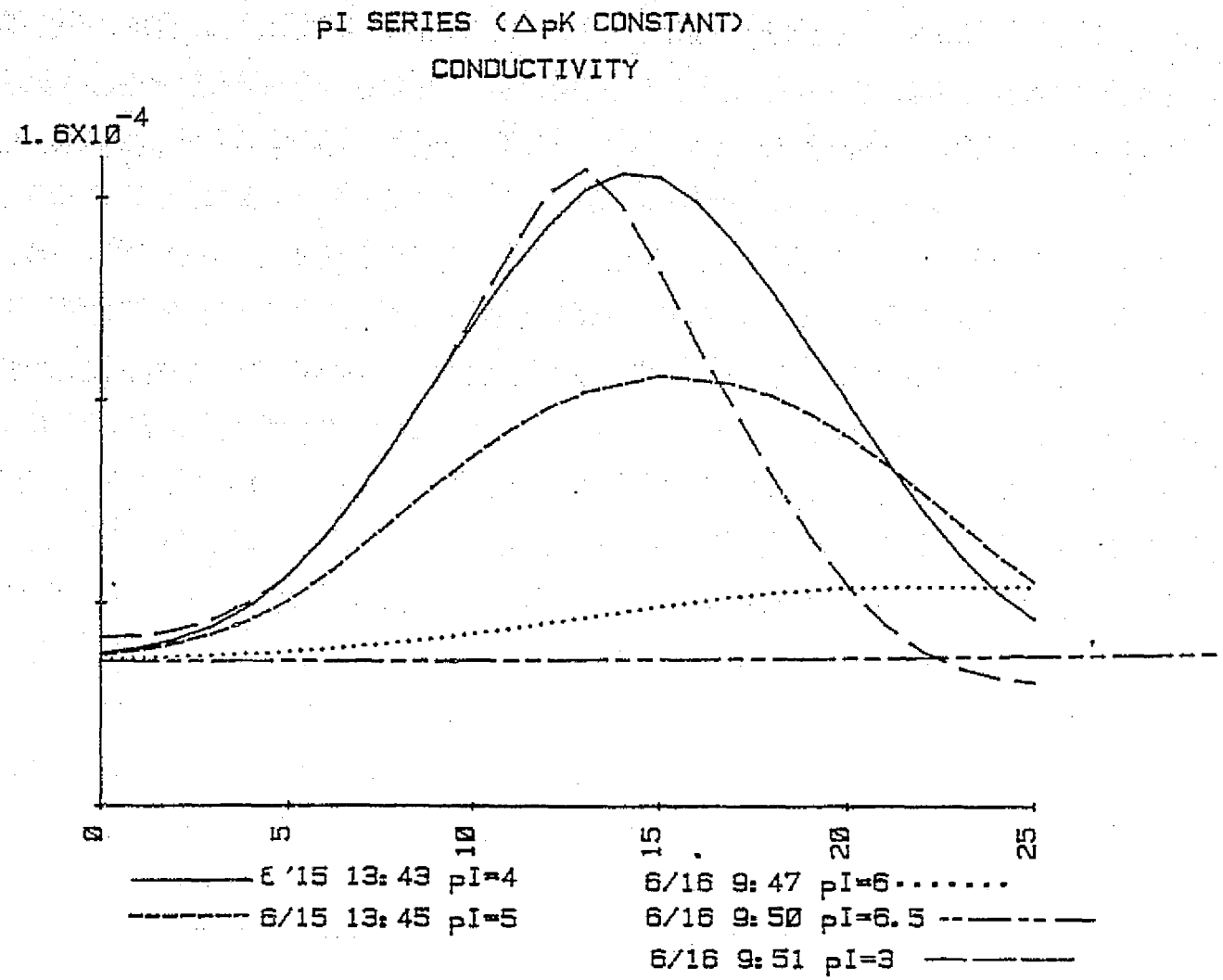

Fig. 4: The conductivity profiles generated using one component with a pI of 7, while the pK's of the other component were varied so that the pI ranged from 3 to 6.5.

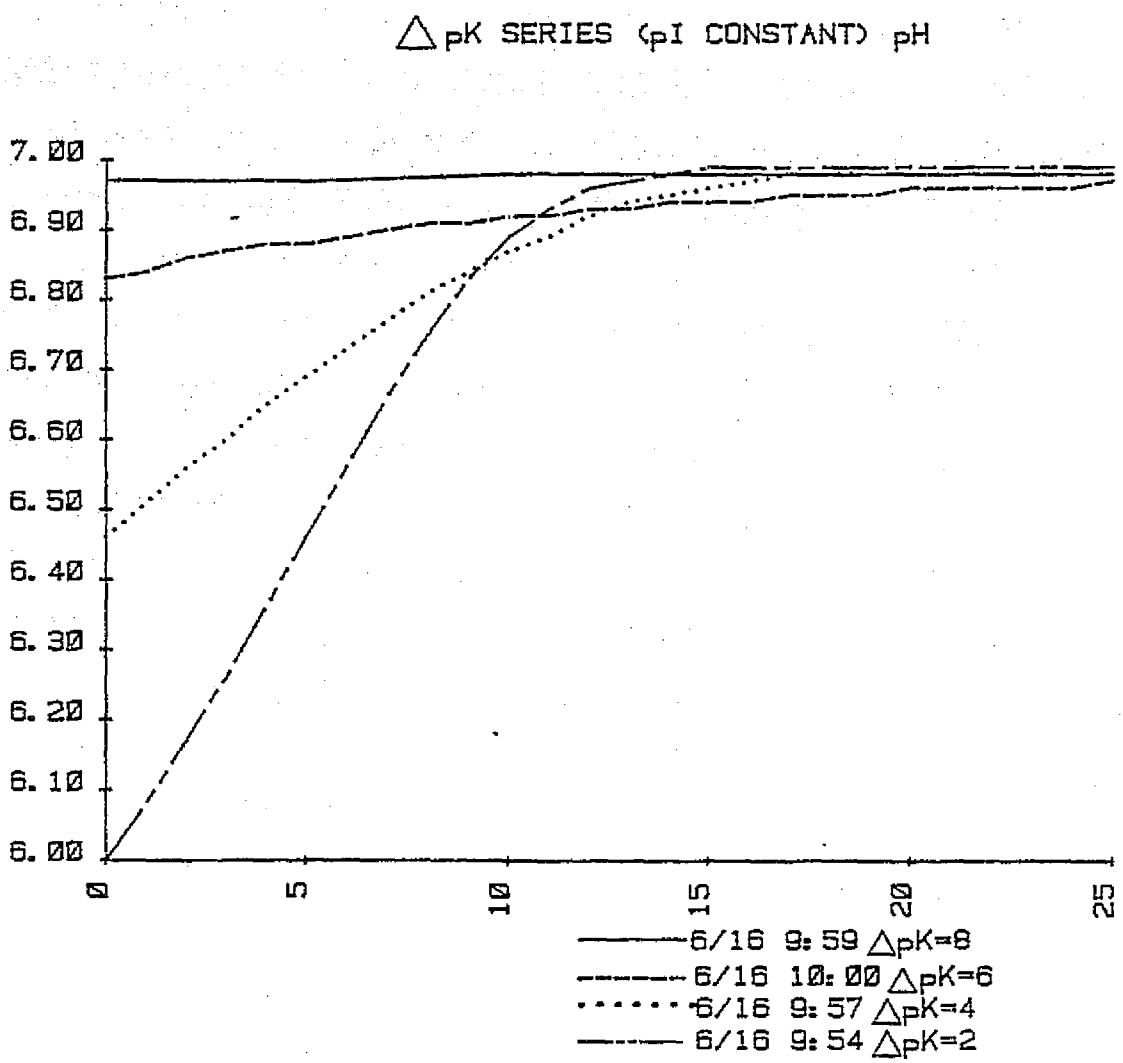

Fig. 5: The pH profiles generated by holding the pK's of one component constant (pK_{B1}=6 and pK_{B2}=8), while the pK's of the other component (pI=5) were varied so that the value of $pK_{A2} - pK_{A1}$ ranged between 2 and 8. The current employed was $4x10^{-7}$A.

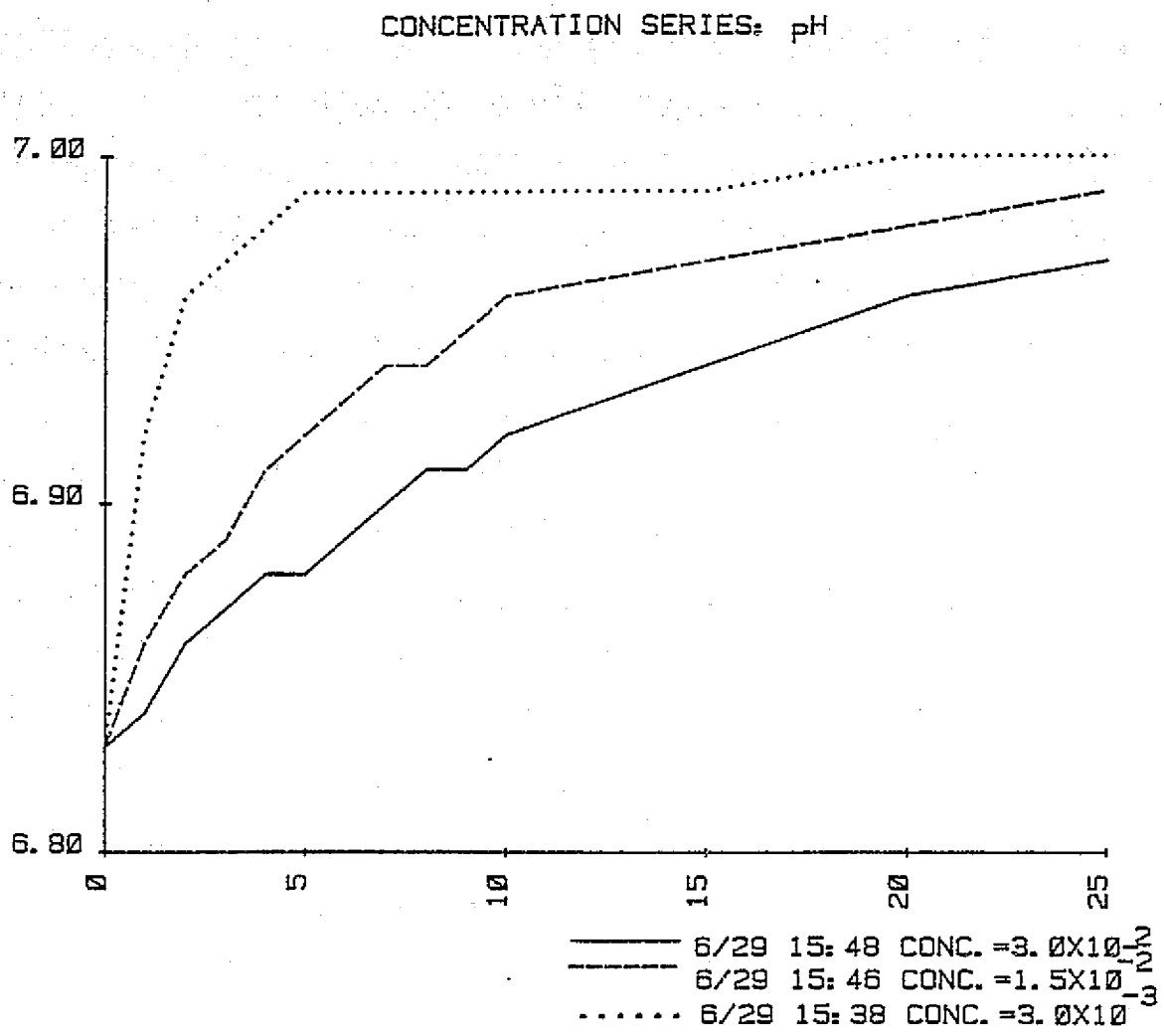

Fig. 6: The pH profiles generated by varying the equal boundary concentrations (molar) of both components.

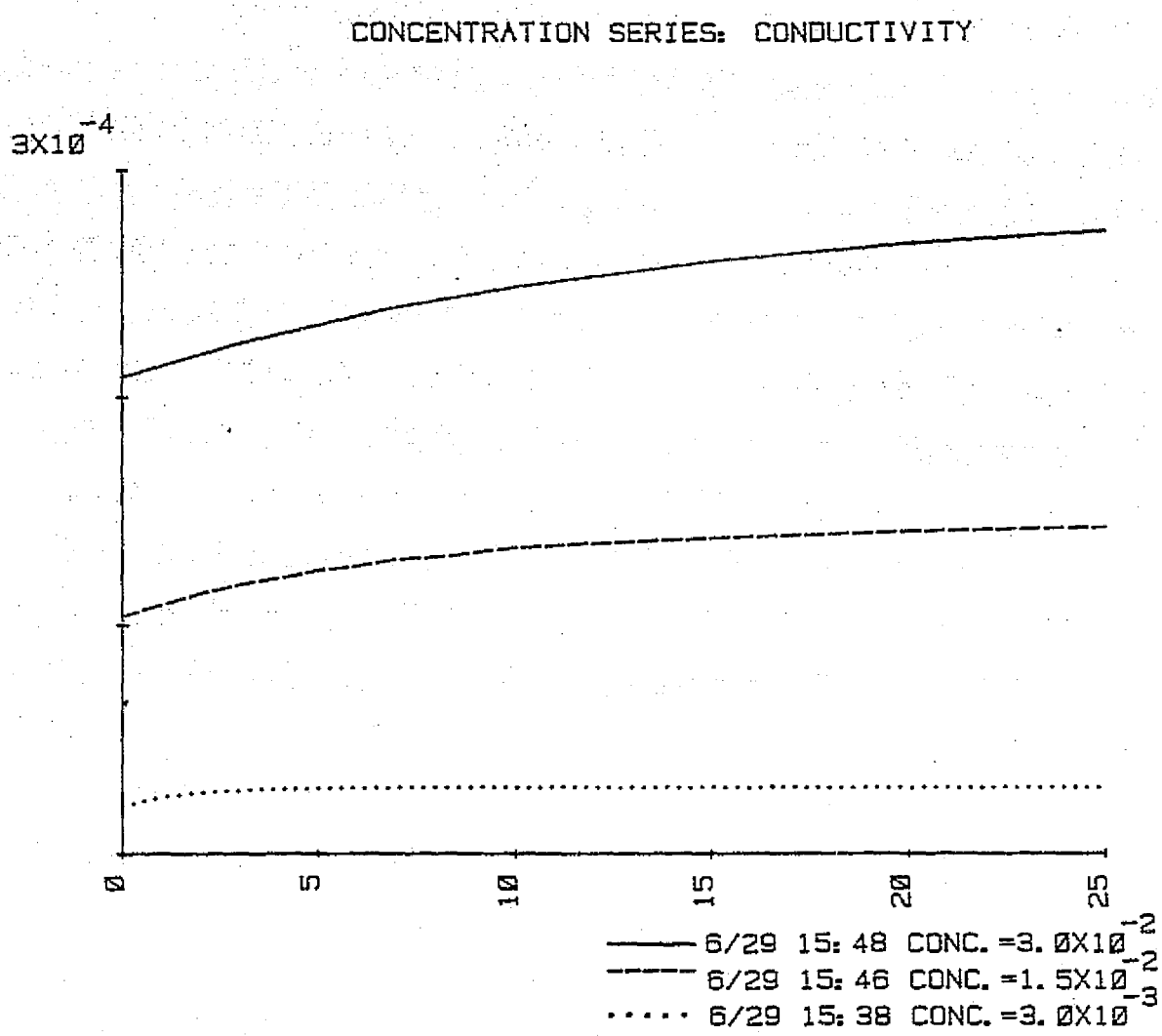

Fig. 7: The conductivity profiles generated by varying the equal boundary concentrations (molar) of both components.

different amperages is demonstrated in figure 8, which gives the concentration profiles of two ampholytes representing glutamic acid and histidine from an equal concentration position. To extend the boundary over 20 cm requires a current of approximately 0.4 microamp. With a current of one milliamp the boundary width is reduced to approximately 0.1 mm. Thus at one milliamp the focused system is essentially an isoelectric zone of glutamic acid contiguous to an isoelectric zone of histidine through a very sharp boundary expressed as a pH discontinuity. The sharp separation in this system more closely resembles an isotachophoretic separation than the type of separation commonly thought to occur in IEF. At comparable amperage when the intermediate component of a three-component system is present in excess of the two end components, an isoelectric zone in the middle of the column results. This isoelectric zone is expressed as both a pH plateau and a conductivity gap. This phenomenon is illustrated graphically in figures 9 and 10. The concept of ampholyte concentration profiles resembling bell-shaped curves[1] is clearly incorrect in this instance. A non-Gaussian ampholyte concentration profile and conductivity gap have been observed experimentally in other laboratories when modifying Ampholine gradients by amino acid addition[5].

2.2. Direction of Continuing Research.

Obviously since these simulations were conducted using the early model based on the electroneutrality approximation, the important aspects of the systems need to be reevaluated through simulations using the revised model.

To date the simulated systems have been evaluated only qualitatively,

[5] see for example, R. K. Brown, M. L. Caspers and S. N. Vinogradow, Carrier Ampholyte Distribution, in Electrofocusing and Isotachophoresis (eds. B. J. Radola and D. Graesslin) pp. 87-96, de Gruyter (1977)

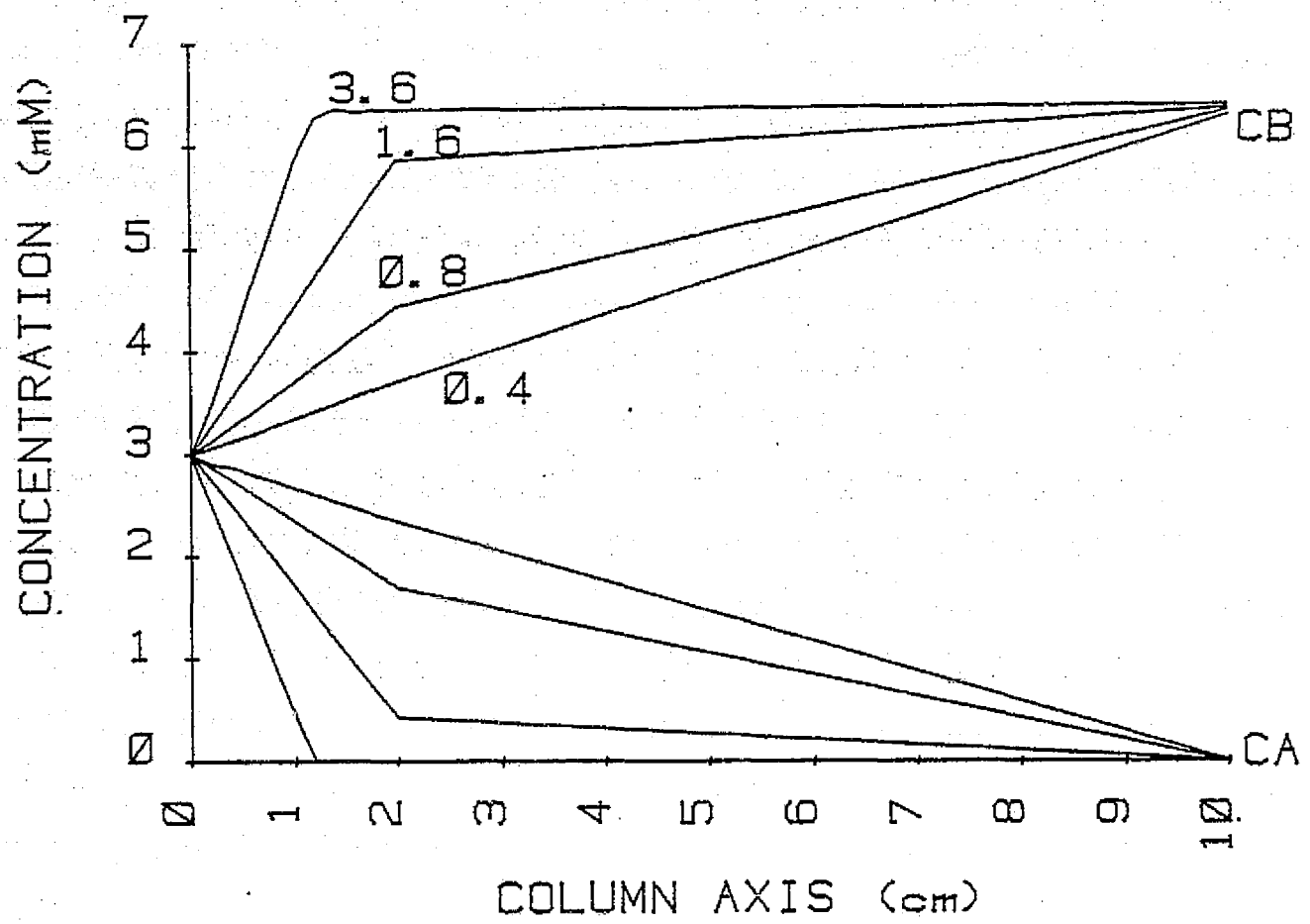

Fig. 8: The concentration profiles of glutamic acid (CA) and histidine (CB) from an equal concentration boundary position. The current was varied from 0.4 to 3.6 microamps.

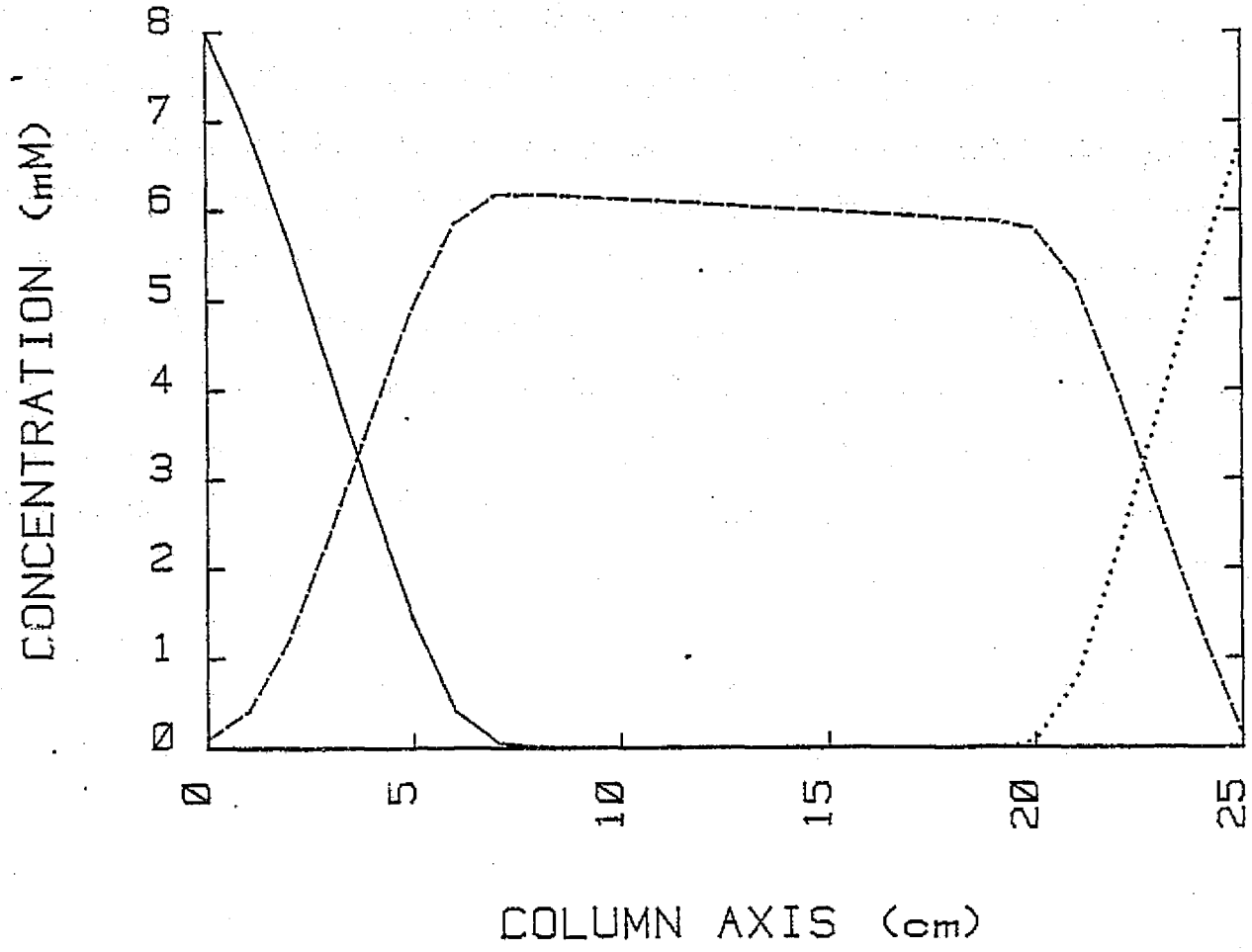

Fig. 9: The concentration profiles of the three-component system using glutamic acid (solid line), histidine (dotted line), and a third component (broken line) with an intermediate pI (pK_1 = 4, pK_2 = 6). The current employed was 1.7x10-6A.

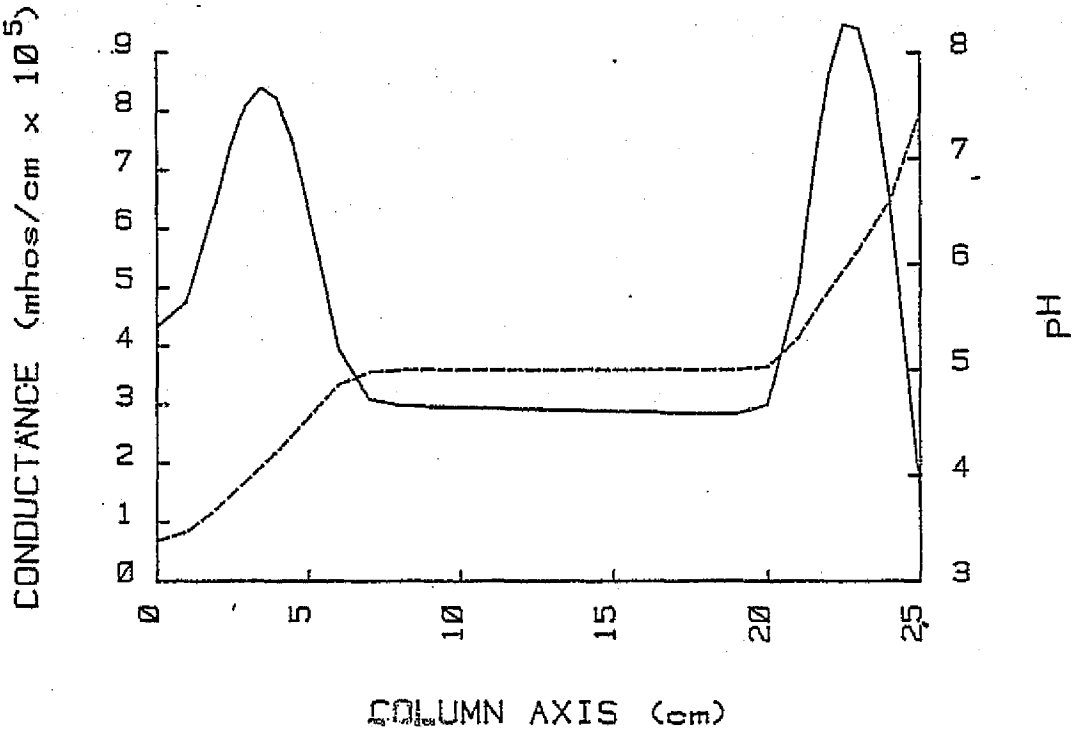

Fig. 10: The conductivity (solid line) and pH (broken line) profiles of the three component system. The ampholytes and conditions are identical to Fig. 9.

i.e., with regard to conductivity, the best gradients are those exhibiting a relatively constant, high conductivity profile; with regard to pH, a linear profile would normally be preferred. It is expected that both narrow and broad range pH gradients are of interest; the narrow range (approximately one pH unit) would be preferred for separations within a specified region such as a preparative purification of a single protein; the broad range pH gradient would be useful analytically or in preparative applications where high resolution is not required.

To quantitatively evaluate focusing systems, one can resort to Rilbe's definition[6] of the resolving power of the method:

$$\Delta pI = 3 \left[\frac{D \ (dpH/dx)}{E \ (-du/dpH)}\right]^{\frac{1}{2}}$$

where ΔpI is the pH difference between just-resolved protein zones, D is the diffusion coefficient of the protein and du/dpH is the slope of mobility vs pH at the component's isoelectric point. This could be applied by establishing a unit or constant value for (D/-du/dpH) and calculating maximum and mean values of ΔpI for each gradient. This of course assumes that the sample ampholytes are in low enough concentration that they have no influence on the established gradient. Alternatively, one of the ampholytes of the model may be given the characteristics of a sample ampholyte, and its distribution in the focusing column evaluated. It would be advantageous to incorporate this type of analysis into the computer program.

[6] H. Rilbe, Ann. N. Y. Acad. Sci. 209, 11-22 (1973)

3. EXPERIMENTAL VERIFICATION OF THE THEORETICAL MODEL

3.1. Experimental Findings.

To confirm the theoretical model, we need accurate profiles of a system focused under several different experimental conditions. Since pH, conductivity, and ampholyte concentration profiles all represent different aspects of the same information, any of these may be utilized. The technique of analysis of course must be capable of discrimination within a small fraction of the length of the established gradient. We do not currently have an experimental setup which provides the requisite resolution, but we have made some qualitative observations.

The most obvious testable prediction of the model is that the boundary between glutamic acid and histidine will be very narrow when the applied current is in the milliampere range. This was tested in two ways using the ISCO column: 1) the column was focused containing only the ampholytes glutamic acid (Glu, pI = 3.22) and histidine (His, pI = 7.58), then fractionated into 0.4 ml fractions (each representing 0.5 cm of column length) and the fractions analyzed; 2) the column was focused containing a visible marker in addition to the carrier ampholytes and isoelectric between them.

In the former method, the fractions were analyzed as to conductivity, amino acid analysis, absorption at 212 nm (histidine absorbance peak), and pH. The absorbance and pH profiles of the column are presented in figures 11 and 12. Although there is considerable loss of resolution during the fractionation procedure, the sharply discontinuous nature of the boundary is well-enough preserved to be illustrated by these data.

When hemoglobin which is isoelectric around pH 7.2 was included

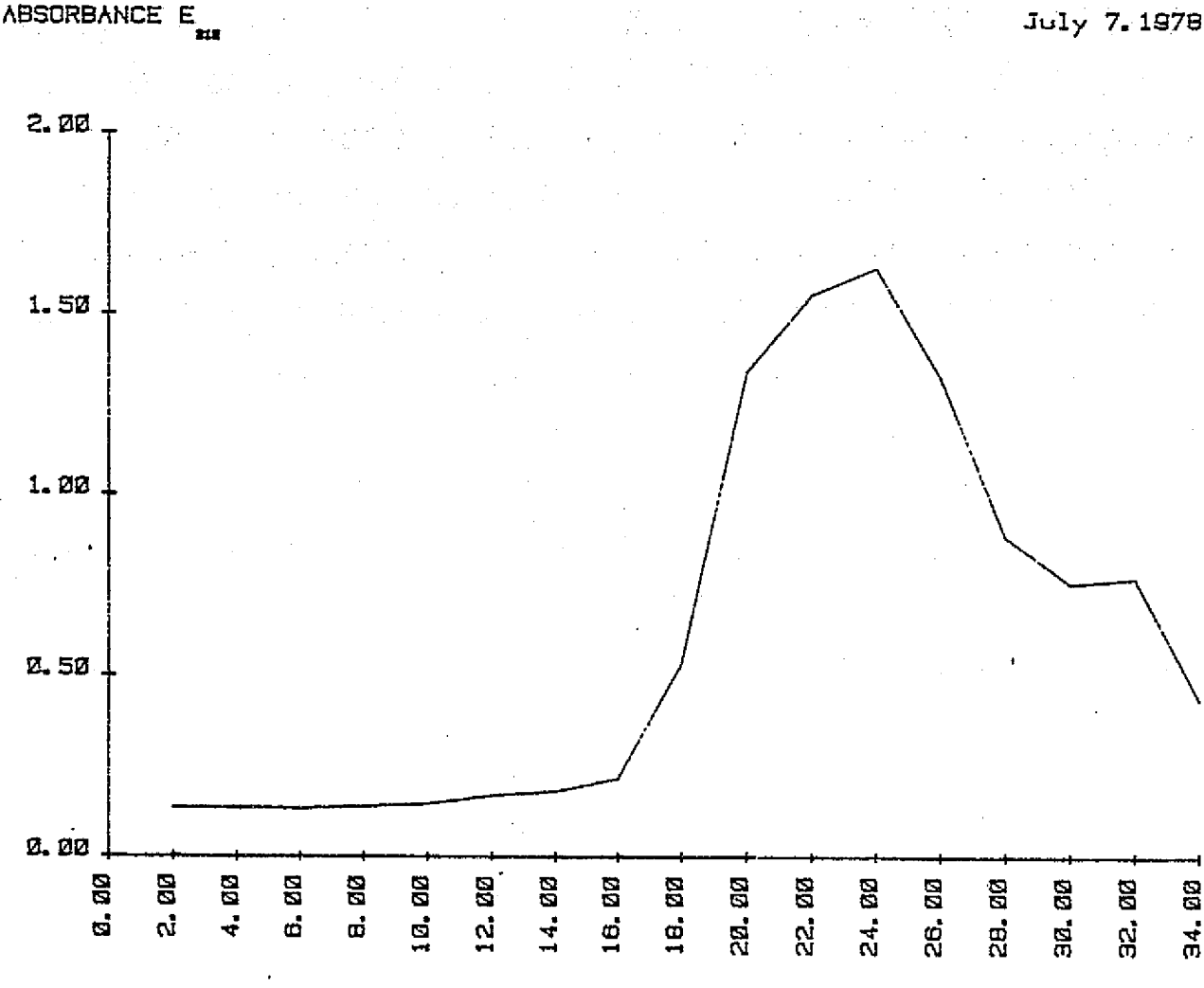

Fig. 11: The absorbance profile at 212 nm of the fractions eluted from a focused column containing the ampholytes glutamic acid and histidine on a sorbitol density gradient. The applied current at steady state was 3×10^{-5}A.

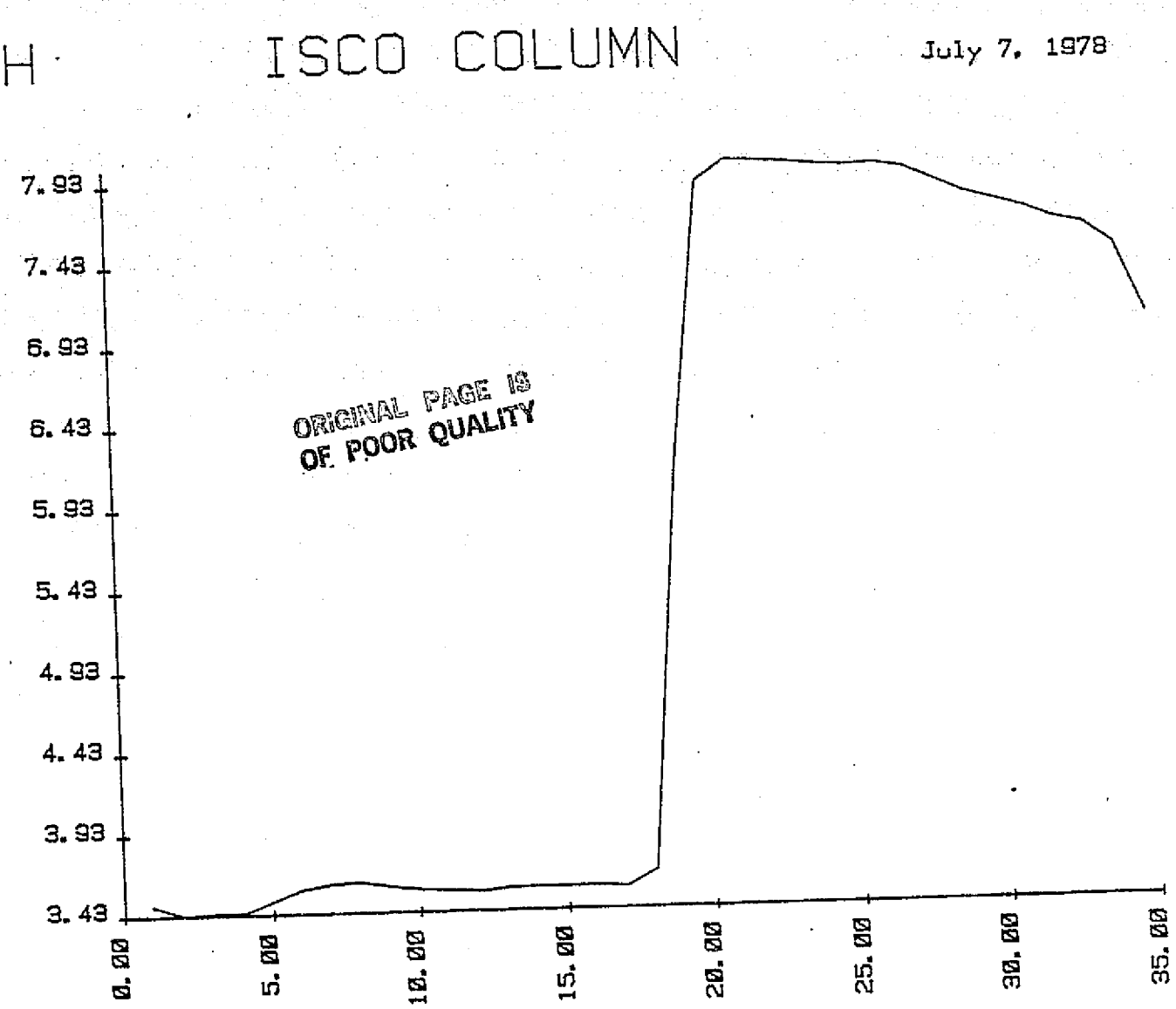

Fig. 12: The pH profile of the fractions eluted from a focused column containing the ampholytes glutamic acid and histidine on a sorbitol density gradient.

in the column as a visible marker, it focused in a very narrow band (less than 2mm wide) at the boundary between the Glu and His zones. When albumin dyed with bromophenol blue (which is isoelectric around pH 5.4) was included, both the hemoglobin and albumin bands were sharp and contiguous. When glycyl-glycine (pI = 5.65) was included as a third carrier ampholyte, the albumin focused between Glu and Gly-gly and the hemoglobin focused between Gly-gly and His in separate narrow bands. This demonstrates the possibility of separation of proteins by interposition or bracketing with carrier ampholytes analogous to mobility bracketing of proteins in isotachophoresis. When methyl red (pI 3.75) was used as a marker between His and Glu, it focused into a narrow band whose top half was red (the acidic color of methyl red) and whose bottom half was yellow (the dye's basic color). This strikingly demonstrated the very steep pH gradient occuring within the narrow boundary. While these data are qualitative rather than quantitative, they illustrate the discontinuous nature of the boundary between adjacent ampholytes in this system.

3.2. Direction of Continuing Research.

To facilitate gathering the accurate profile data required to confirm the validity of the model, we are in the process of designing a system which will allow analysis along the length of a IEF column without requiring fractionation. Two types of apparatus are being considered: 1) a scanning conductivity probe which would move axially within the focusing column, and 2) a column capable of being scanned along its length in a spectrophotometer. The latter would utilize a small column contained within the lumen of a temperature-

jacketed, quartz, flow-through cell (Hellma 167-QS). We have conducted preliminary focusing experiments in the Hellma cell and achieved satisfactory results.

4. IMPLEMENTATION OF SIMPLE AMPHOLYTE IEF FOR PROTEIN SEPARATIONS

4.1. Results to Date.

We have seen that simple ampholytes can be focused so that the boundaries between adjacent components are either broad, giving a pH gradient, or narrow, giving a pH step. Broad boundaries are favored by low fields, high ampholyte concentrations, high values of $pK_2 - pK_1$ for biprotic ampholytes, and small differences in the isoelectric points of neighboring ampholytes, i.e., $pI_B - pI_A$. The converse of these conditions favors narrow boundaries.

A pH-step system can be used to space or bracket specific proteins; however, the resolution of this technique is dependent upon the availability of ampholytes with closely spaced isoelectric point since an ampholyte of intermediate pI is required to separate sample proteins. To display a resolving power of 0.02 pH units would require 50 components with pI's spaced over a single pH unit. This sort of system is perhaps already available in the form of Ampholine, although the number of Ampholine components used and their relative concentrations are of course not amenable to adjustment. Bracketing with high resolution using a reasonable number of components is probably more easily achievable in isotachophoresis than in IEF, since mobility is a flexible property for weak electrolytes and may be altered with pH, whereas isoelectric points are essentially inflexible. Bracketing with low resolution could conceivably be useful for separating a complex mixture into specific subgroups; however, it does not appear that such a technique would be of general

usage.

The use of pH-gradient systems is the alternative to using pH steps, and we have begun to explore this alternative experimentally. In our preliminary attempts to focus proteins on simple ampholyte pH gradients we have primarily used a polyacrylamide slab gel system. The slab gels are easily manipulated and multiple gels can be run simultaneously. We have chosen to setup shallow, narrow-range pH gradients using two or three amino acids or dipeptides as carrier ampholytes. To date we have conducted experiments in only a few systems using the following amino acids and peptides: aspartic acid (pI = 2.77), glutamic acid (3.22), histidyl-glycine (6.81), histidyl-histidine (7.30), glycyl-histidine (7.50), histidine (7.59), and β-alanyl-histidine (8.17). The goal of these preliminary experiments was to determine if proteins can be focused with high resolution on a pH gradient formed from only two or three components. For sample proteins we have used hemoglobin (Hb), catalase (Cat), or fractions of dialyzed egg protein (ED). After focusing a strip of the gel is removed and sectioned, each section is eluted and the pH of the eluate recorded. The remainder of the gels are fixed with a Coomasie Blue solution to allow visualization of the proteins. Protein distributions on representative gels and their pH profiles are presented as figures 13 through 18. The pH range of the gel usually exceeds the pI range of the ampholytes, i.e. the focusing column escapes ampholyte control at the ends. This phenomenon apparently is caused by the presence of buffers and salts in the system (by products of the acrylamide polymerization reaction), and the magnitude of the effects is reduced by increasing ampholyte concentrations. While these results are very

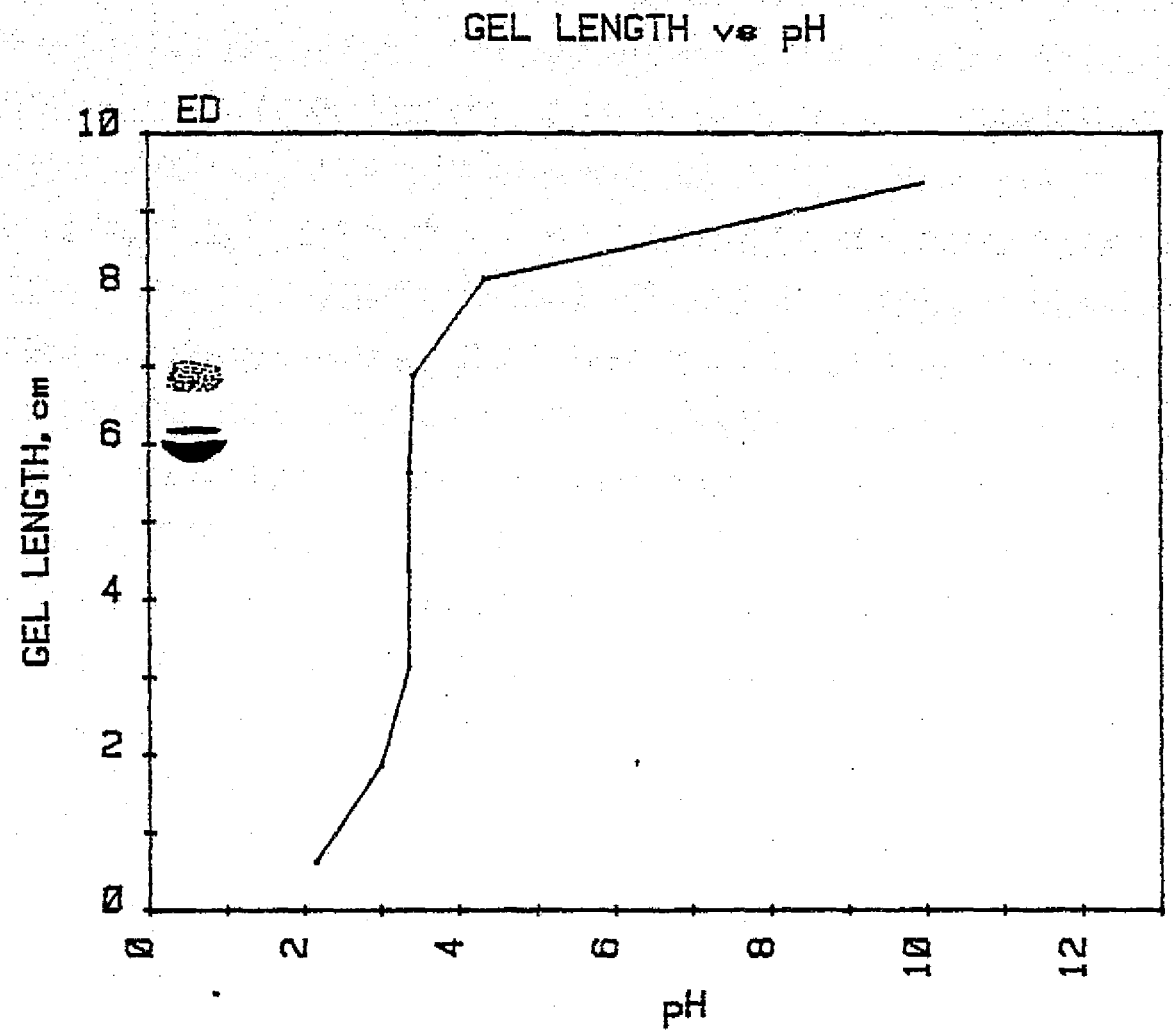

Fig. 13: The pH profile of an aspartic acid and glutamic acid gel with sample of egg white protein.

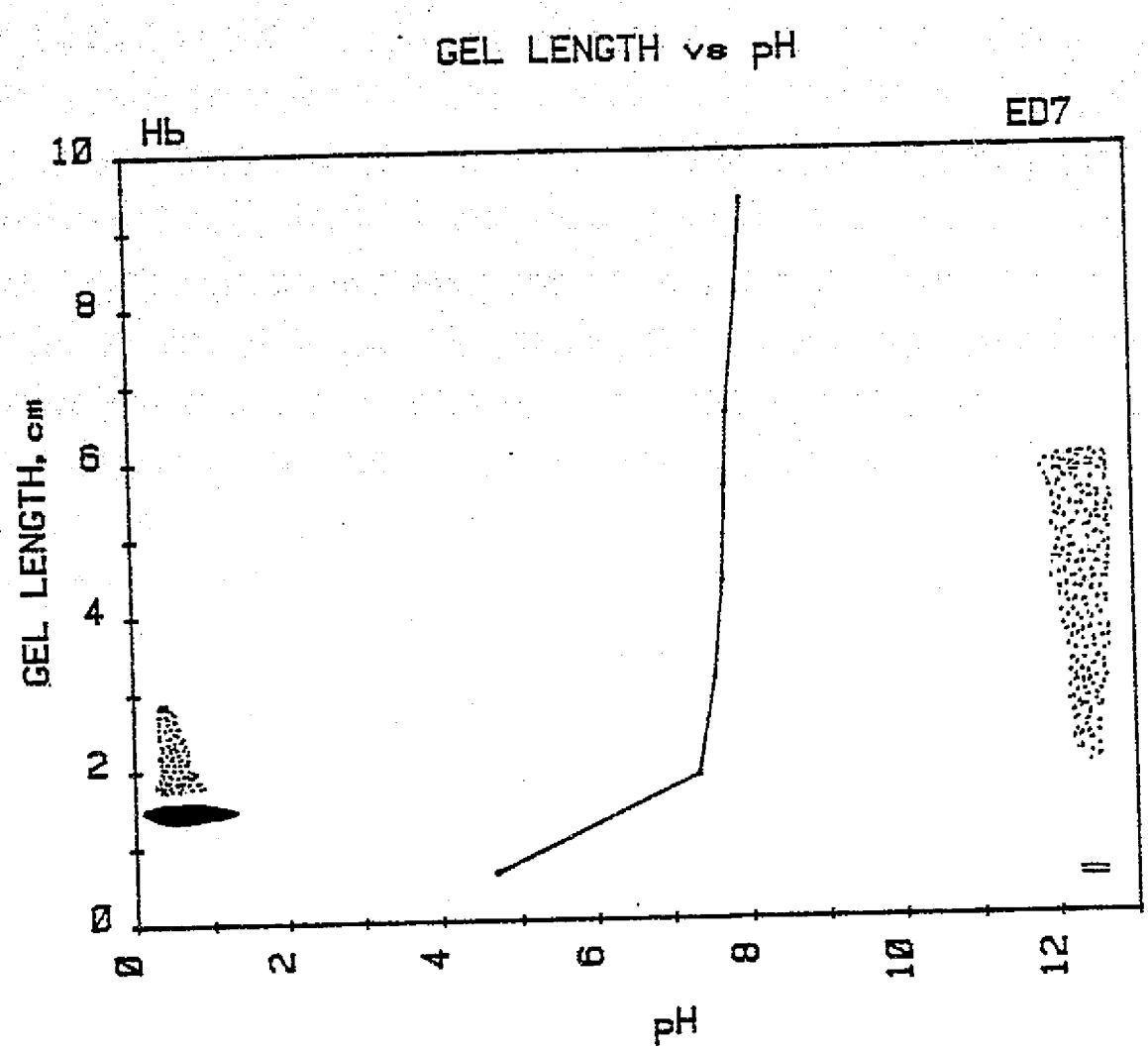

Fig. 14: The pH profile of a histidyl-histidine and alanyl-histidine gel with samples of hemoglobin and egg white protein fraction.

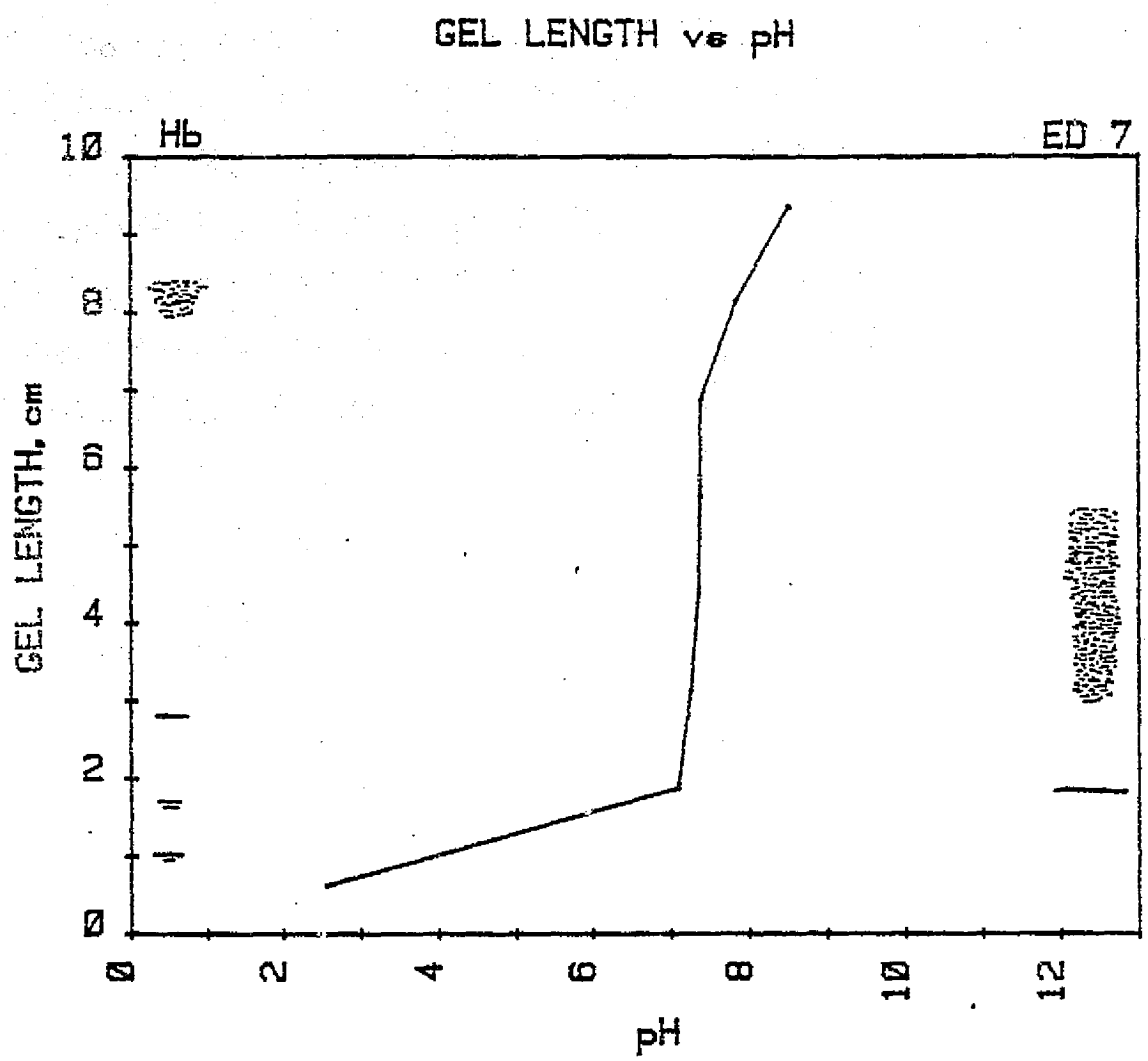

Fig. 15: The pH profile of a histidyl-glycine and alanyl-histidine gel with samples of hemoglobin and egg white protein fraction.

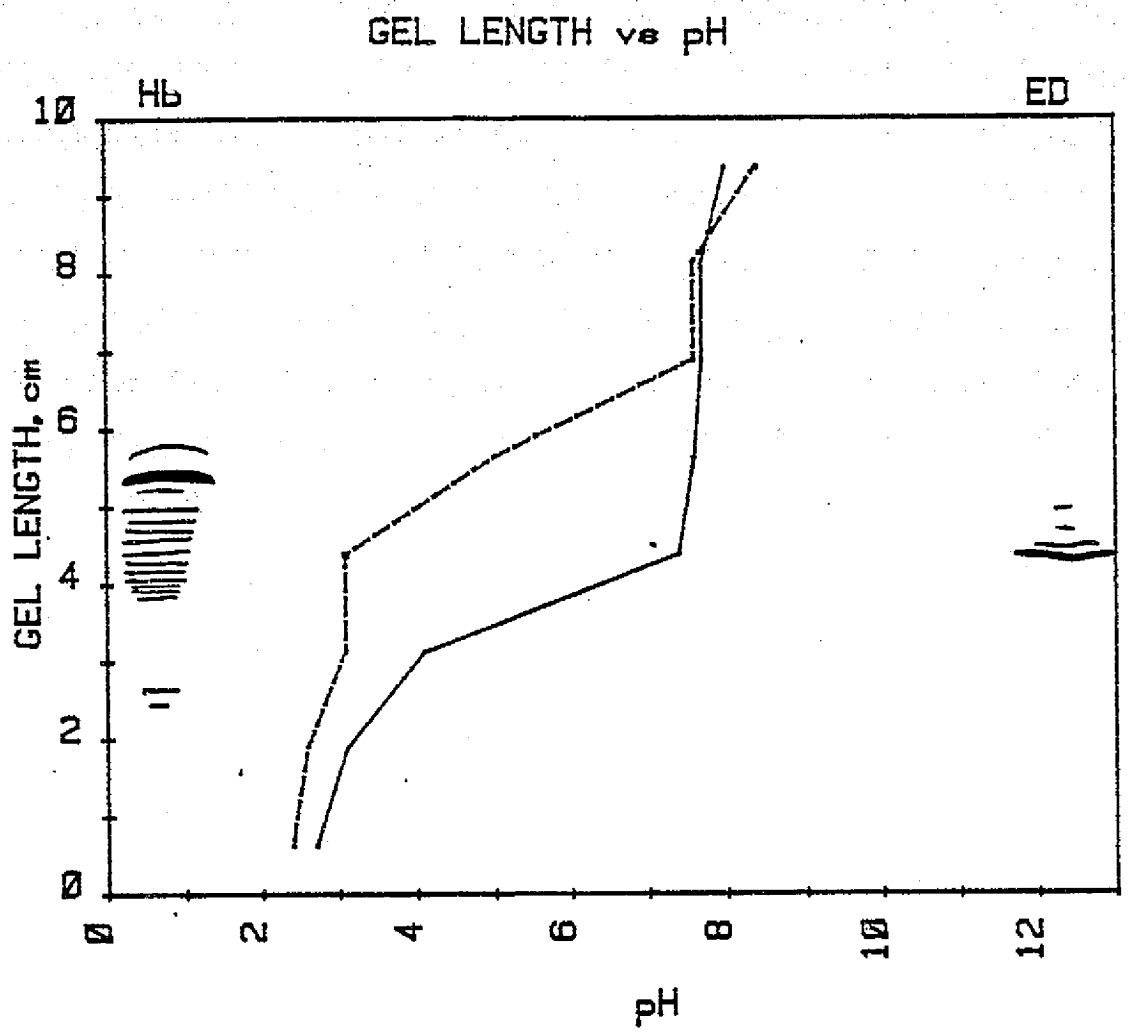

Fig. 16: The pH profile of a glycyl-histidine and alanyl-histidine gel with samples of hemoglobin and egg white protein.

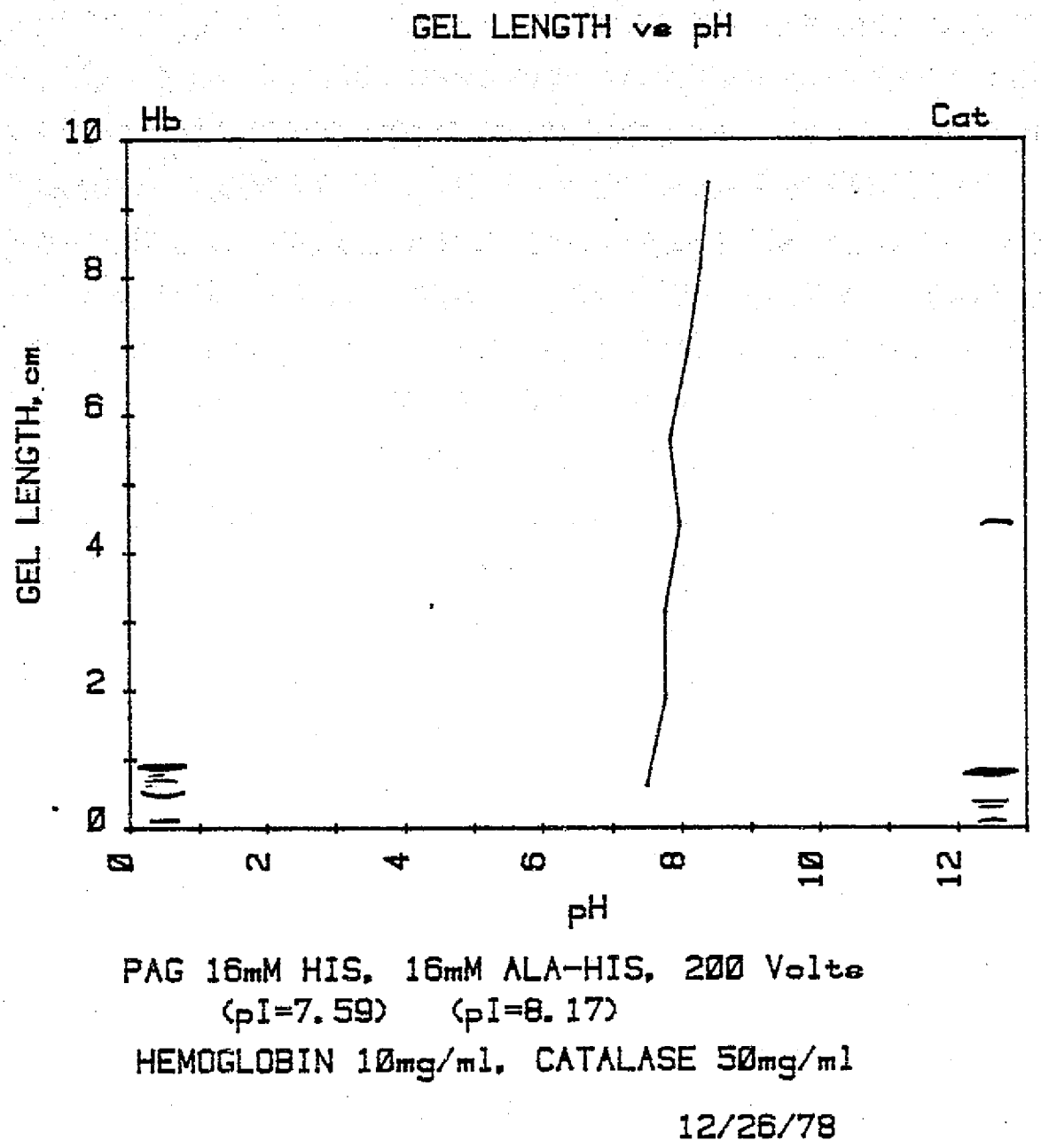

Fig. 17: The pH profile of a histidine and alanyl-histidine gel with samples of hemoglobin and catalase.

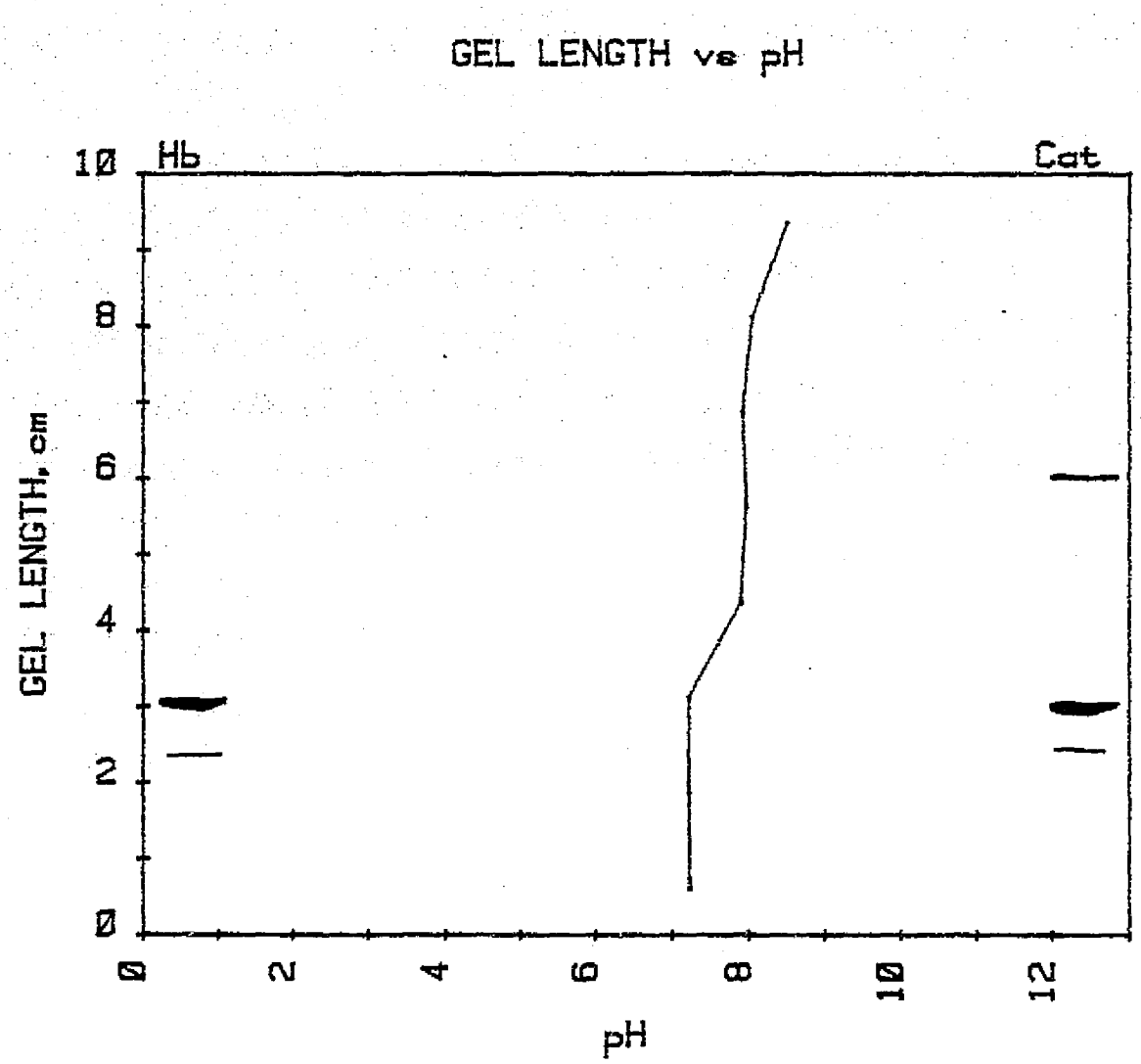

Fig. 18: The pH profile of a histidyl-glycine, histidine, and alanyl-histidine gel with samples of hemoglobin and catalase.

preliminary, the separations observed in some systems are quite good (see hemoglobin in figures 15-17 and catalase in figure 17), and indicate that it is possible to focus proteins on a pH gradient formed with only two or three simple ampholytes.

4.2. Direction of Continuing Research.

For simple ampholyte IEF to be of maximum utility in protein separations, three types of focusing systems should be developed. In order of developmental priority they are: first, narrow-range focusing systems, which collectively span the pH range from 2 to 11 and individually cover a single pH unit utilizing a small number of simple ampholytes; second, a broad-range focusing system, which by itself covers the pH range from 2 to 11; third, a flexible method of designing custom-tailored pH gradients to fit specific and unusual separation problems. Our goal is to develop all three types of systems in forms suitable for both analytical and preparative application.

APPENDIX A

THEORY AND COMPUTER SIMULATION OF ISOELECTRIC FOCUSING WITH SIMPLE AMPHOLYTES

ELECTROFOCUS/78

Abstract Form

(Space for typing abstract)

THEORY AND COMPUTER SIMULATION OF ISOELECTRIC FOCUSING WITH SIMPLE AMPHOLYTES, T. T. Allgyer, O. A. Palusinski, and M. Bier, Biophysics Technology Laboratory, University of Arizona, Tucson, Az. 85721

The objective of the present study is to develop a mathematical description of an Ampholine-free, multicomponent, isoelectric focusing system in the steady state, i.e., to obtain the means of computing ampholytes' concentrations, the pH, conductance, and related parameters at every point along the column axis in terms of the components' mobilities, diffusion coefficients, and proton dissociation constants.

The fundamental principles describing the components' chemical equilibria, the mass transfers resulting from diffusion and electromigration, and electroneutrality were used to provide a model consisting of ordinary differential equations coupled with an algebraic equation. The model equations were solved using discretization techniques based on the Runge-Kutta-Merson integration rule. The method of solution was implemented on a digital computer using FORTRAN-based simulation software. The program provides the desired information in a convenient graphic form. Computer-generated concentration, pH, and conductance profiles for arbitrary two and three-component systems are presented, and the complete mathematical model of the three-component system is given.

This work represents preliminary steps in the development of a general mathematical model for steady-state isoelectric focusing. The results presented indicate that the approach chosen may be successfully employed in the formulation of the model and its subsequent solution. The model generalized to the level of n-components will provide a basic tool for the design and optimization of isoelectric focusing systems using simple ampholytes.

Name(s) of author(s)

T. T. Allgyer, O. A. Palusinski, and M. Bier

Mailing address of first author: Biophysics Technology Laboratory, University of Arizona, Pharmacy/Microbiology Bldg. #90

City/State/Zip Tucson, Arizona 85721

Please read instructions on reverse before using this form.

INTRODUCTION

In isoelectric focusing (IEF) a stable pH gradient is created by electrophoretic migration of carrier ampholytes to stationary positions in the separation column. Ampholytic sample components introduced in the system distribute themselves on the pH gradient so that they exhibit concentration maxima at their respective isoelectric points. In regards to the processes which determine their distribution on the column, the distinction between carrier ampholytes and sample ampholytes is purely semantic.

The existing theory of steady-state IEF is attributable to Svensson[1] and was developed in conjunction with the introduction of the technique. Svensson addressed the one-component system, i.e., the concentration distribution of a pure end component; and also the concentration distribution of an ampholytic component added to a system whose pH and conductance are known as a function of the distance along the separation axis. Such systems were rendered possible by Vesterberg's development of a random mixture of carrier ampholytes[2], commercially introduced under the trade name of Ampholine.[3] Their ready availability assured the remarkable growth of the various IEF techniques, but also rendered unnecessary further development of the theory of steady-state IEF. There have been no significant contributions to this theory since Svensson.

Recent attempts to develop alternate means of forming stable natural pH gradients [4-7] have been based on a purely empirical approach. We feel that this goal would be furthered by the development of an explicit mathematical theory of multiple ampholyte IEF. This paper represents our approach in this direction, and we hope that it will contribute to an understanding of the theoretical basis of IEF.

MODEL FORMULATION

The construction of a mathematical model of IEF is based upon the following concepts:

a. the concentration of component subspecies are described by equations of chemical equilibria,

b. in the steady state, a balance exists between the mass transports resulting from electromigration and from diffusion,

c. the condition of electroneutrality prevails as a first approximation, and

d. the current density is constant throughout the separation column. The specific goal of the present theoretical treatment is to develop a mathematical description of a multicomponent IEF system at every point along its axis, i.e., to obtain the component concentrations, pH, conductance, and related parameters specified in terms of the components' mobilities, diffusion coefficients, and proton dissociation constants.

The theoretical treatment presented here assumes a good measure of ideality, specific assumptions were as follows: (1) a negligible contribution of H^+ and OH^- to the conductance within the pH range of interest, (2) only the two apparent dissociation constants (pK's) nearest the isoelectric point (pI) of an ampholyte exert significant influence upon its behavior in the steady state, (3) component subspecies have only a single absolute ion mobility, and (4) electroosmosis and radial and longitudinal temperature gradients are not significant.

FUNDAMENTAL RELATIONS

The equations have been developed for both the two and three-component systems. The three-component system is used to illustrate the fundamental relations. The concepts and treatment are generally applicable, and generalized

forms of the critical equations are given below in the discussion of the method used in solution of the equations in computer simulation.

The concentrations of component subspecies can be expressed in terms of the total concentration C_i of that component and the hydrogen ion concentration h:

$$C_i^+ = \frac{h^2 C_i}{(h^2 + hK_{i1} + K_{i1}K_{i2})} \tag{1}$$

$$C_i^- = \frac{K_{i1}K_{i2}C_i}{(h^2 + hK_{i1} + K_{i1}K_{i2})} \tag{2}$$

$$C_i^o = \frac{hK_{i1}C_i}{(h^2 + hK_{i1} + K_{i1}K_{i2})} \tag{3}$$

where i may be a, b, or c representing the three components of the system; C_i^+ is the concentration of cationic ampholyte; C_i^-, the anionic ampholyte; and C_i^o, the uncharged and zwitterionic ampholyte. K_{i1} and K_{i2} are the first dissociation constants of the ampholyte when titrated from the isoelectric state with acid and base respectively.

At any point the net mass transfer of each component resulting from electromigration can be described in terms of the charged subspecies concentrations as

$$J_e^i = \frac{I}{q\kappa} u_i (C_i^+ - C_i^-) \tag{4}$$

where I is the current (amperes); q, the cross-sectional area (cm^2); κ, the conductance (mhos cm^{-1}); and u_i, the component mobility (cm^2 $volt^{-1}$ sec^{-1}).

The conductance is given by

$$\kappa = F/1000 \{ u_a(C_a^+ + C_a^-) + u_b(C_b^+ + C_b^-) + u_c (C_c^+ + C_c^-) \} \quad (5)$$

where F is the Faraday constant and the component subspecies concentrations are molar.

At any point the diffusional mass transport of each component is described as

$$J_d^i = -D_i \, dC_i/dx \quad (6)$$

where D_i is the diffusion coefficient (cm^2 sec^{-1}) and x is the independent variable representing the distance along the column. Since in the steady state the net mass transport of a chemical component resulting from electromigration must balance the transport from diffusion, we can write

$$J_e^i = -J_d^i \quad (7)$$

and using equations (4) and (6), this becomes

$$dC_i/dx = \frac{I}{D_i q \kappa} u_i \, (C_i^+ - C_i^-) \quad (8)$$

Taking into account equations (1) and (2) we obtain explicit form of the equations:

$$dC_a/dx = \frac{1000I}{D_a qF} \frac{u_a C_a (h^2 - K_{a1}K_{a2})}{(h^2 + hK_{a1} + K_{a1}K_{a2})} \frac{1}{\phi}$$

$$dC_b/dx = \frac{1000I}{D_b qF} \frac{u_b C_b (h^2 - K_{b1}K_{b2})}{(h^2 + hK_{b1} + K_{b1}K_{b2})} \frac{1}{\phi} \quad (9)$$

$$dC_c/dx = \frac{1000I}{D_c qF} \frac{u_c C_c (h^2 - K_{c1}K_{c2})}{(h^2 + hK_{c1} + K_{c1}K_{c2})} \frac{1}{\phi}$$

where the function ϕ has the form:

$$\phi = \frac{u_a C_a (h^2 + K_{a1}K_{a2})}{(h^2 + hK_{a1} + K_{a1}K_{a2})} + \frac{u_b C_b (h^2 + K_{b1}K_{b2})}{(h^2 + hK_{b1} + K_{b1}K_{b2})} + \frac{u_c C_c (h^2 + K_{c1}K_{c2})}{(h^2 + hK_{c1} + K_{c1}K_{c2})} \quad (9a)$$

The electroneutrality condition for the three-component system may be stated as

$$h + C_a^+ + C_b^+ + C_c^+ = K_w/h + C_a^- + C_b^- + C_c^- \quad (10)$$

where K_w is the ion product of water.

NUMERICAL SOLUTION AND COMPUTER IMPLEMENTATION

We present briefly the discretization procedure of the model equations, the numerical integration technique, and the computer implementation of the model.

It is convenient to write the differential equations for C_a, C_b and C_c concentrations in the form:

$$dC_a/dx = \frac{1000I}{D_a qF} f_a(C_a, C_b, C_c, h)$$

$$dC_b/dx = \frac{1000I}{D_b qF} f_b(C_a, C_b, C_c, h) \quad (11)$$

$$dC_c/dx = \frac{1000I}{D_c qF} f_c(C_a, C_b, C_c, h)$$

where f_a, f_b, f_c are the functions specified in relation (9). The functions f_a, f_b, f_c satisfy the Lipschitz condition with respect to all arguments. Using equations (1) and (2) we can write equation (10) in the form of a polynomial:

$$\sum_{j=o}^{8} b_{j+1} h^j = 0 \quad (12)$$

where $b_9 = 1$.

The coefficients b_j of the polynomial are linear functions of C_a, C_b, C_c of the form

$$b_j = b_{jF} + b_{ja}\, C_a + b_{jb}\, C_b + b_{jc}\, C_c \tag{13}$$

and the parameters b_{jF}, b_{ja}, b_{jb}, b_{jc} depend on the dissociation constants K_{ak}, K_{bk}, K_{ck} (k=1,2), and the ion product of water K_w. These coefficients are presented explicitly in the Appendix. The solution of system (11)(12), which consists of differential and algebraic equations[8], is in general not unique. The uniqueness is guaranteed by picking one specific root of the polynomial. This has to be based on physical considerations.

The differential equations (11) were discretized using the Runge-Kutta-Merson scheme[9], which can be described as follows:

$$\begin{aligned} C_{an+1} &= C_{an} + \Delta x_n\, \psi_a\, (C_{an}, C_{bn}, C_{cn}, h_n, \Delta x_n) \\ C_{bn+1} &= C_{bn} + \Delta x_n\, \psi_b\, (C_{an}, C_{bn}, C_{cn}, h_n, \Delta x_n) \\ C_{cn+1} &= C_{cn} + \Delta x_n\, \psi_c\, (C_{an}, C_{bn}, C_{cn}, h_n, \Delta x_n) \end{aligned} \tag{14}$$

where

$\Delta x_n = x_{n+1} - x_n$ is the integration stepsize.

The functions ψ_a, ψ_b, ψ_c specified by the chosen discretization are computed using the right sides of equations (11). The subscript n added to the variables in the above equation indicates the discrete values corresponding to the value of the independent variable x

$$x_n = x_o + \sum_{i=o}^{n-1} \Delta x_i \tag{15}$$

where x_o is the initial value.

The coefficients b_j of the polynomial (12) are computed for each step x_n based upon the values C_{an}, C_{bn} and C_{cn}. Then the roots are extracted using the Newton-Raphson iterative technique. Having computed the roots we select the real positive root(s). When there is more then one positive real root, the root closest to the former value of h_{n-1} is substituted for h_n. When there is no real positive root the former value of h_{n-1} is retained. This procedure can be described as follows:

$$h_n = \min_{|r_k - h_{n-1}|} \{r_k;\ Re(r_k) > 0 \wedge Im(r_k) = 0\} \tag{16}$$

where $Re(r_k)$ is the real part of the root r_k, and $Im(r_k)$ is the imaginary part of the root $r_k (k=1,2,\ldots,8)$; $h_n = h_{n-1}$ if the above set is empty.

The program for numerical integration of system (11)(12) was prepared using FORTRAN based simulation software DAREP[10] available at the University of Arizona. The program was implemented on the CYBER 175 digital computer. The polynomial (12) is solved by the subroutine called at each integration step. The subroutine extracts the roots, tests them and substitutes appropriate value for h_n following the formula (16). When there are multiple real positive roots or there is none, an appropriate message is printed out. The integration is performed from the initial value x_o until an end value $x = x_{max}$. The step size Δx_n is automatically controlled by the Runge-Kutta-Merson integration subroutine to maintain local truncation errors within assigned bounds. We assumed relative errors of $10^{-3} - 10^{-5}$. In the cases studied the polynomial displayed only one positive real root which was therefore the only root realistically acceptable. The selection of this root of the polynomial at each integration step guarantees the uniqueness of the solution.

RESULTS

The model was exercised at the level of the two-component system by using values for mobilities, diffusion coefficients, and dissociation constants representative of glutamic acid and histidine. The constants assumed in the calculations are reported in Table I. The separation column was assumed to be 25 cm in length and of 0.79 cm^2 cross-sectional area. The anode was positioned at the top of the column and the cathode at the bottom. The predictions of the model for the two-component system are illustrated in Figures 1, 2, and 3.

The model was also exercised at the level of the three-component system by again using glutamic acid and histidine, and introducing a third component with an intermediate isoelectric point. The predictions of the model for the three-component system are illustrated in Figures 4, 5, and 6.

DISCUSSION

This work represents preliminary steps in the development of mathematical model for IEF. The results presented indicate that the method of solution chosen is capable of being used successfully. We are in the process of experimentally verifying the model's predictions, and intend to perform parameter identification and remodeling as required. Although we do not believe the assumptions presently employed are unreasonable for preliminary theoretical consideration of the system, a more concrete position may not be assumed prior to experimental evaluation.

The model is being generalized to consider an indefinite number of components. At the level of the n-component system, it will provide a basic tool for the design and optimization of natural isoelectric focusing gradient systems.

Recently a great deal of interest has focused upon the modification of pH gradients established by commercially available carrier ampholytes[4,5] and the generation of natural pH gradients by use of simple mixtures of buffers[6,7]. It is generally appreciated that the quantities of individual ampholytes utilized and their specific characteristics must uniquely determine the shape of the pH gradient established, the sample capacity, and the resolution of separation. It should also be appreciated that the empirical approaches presently employed suffer from the absence of a mature theory of IEF. Significant progress cannot be reasonably expected without the development of a valid theory to accompany the empirical thrust.

The computer simulation presented above has shown that the characteristics of gradients formed using a limited number of well-defined ampholytes will be far more dependent on their concentrations and the field applied than is the case when Ampholine is used. The reduction to practice of such novel buffer systems will be facilitated by the development of the automated data collection apparatus described in another paper in this Volume[14].

This research was supported in part by NASA grant NSG-7333.

REFERENCES

1. H. Svensson, Acta Chem. Scand. 15, 325, 1961.

2. O. Vesterberg, Acta Chem. Scand. 23, 2653, 1969.

3. LKB-Produkter AB, Bromma, Sweden.

4. M. L. Caspers, Y. Posey, and R. K. Brown, Anal. Biochem. 79, 166, 1977.

5. R. K. Brown, M. L. Caspers, and S. N. Vinogradow, in "Electrofocusing and Isotachophoresis", B. J. Radola, and D. Graesslin (eds.), Walter de Gruyter, Berlin, 1977.

6. N. Y. Nguyen, D. Rodbard, P. J. Svendsen, and A. Chrambach, Anal. Biochem. 77, 39, 1977.

7. M. L. Caspers, and A. Chrambach, Anal. Biochem. 81, 28, 1977.

8. C. W. Gear, Simultaneous Numerical Solution of Differential Algebraic Equations, IEEE Trans., CT-18, No. 1, 1971.

9. J. D. Lambert, Computational Methods in Ordinary Differential Equations, J. Wiley, N. Y., 1973.

10. J. J. Lucas, J. V. Wait, DAREP - A Portable CSSL-Type Simulation Language, Simulation, 1975.

11. E. J. Cohn, and J. T. Edsall, Proteins, Amino Acids and Peptides, N. Y., 1943.

12. L. G. Longsworth, J. Am. Chem. Soc. 75, 5705, 1953.

13. H. Svensson, Acta Chem. Scand. 16, 456, 1962.

14. M. Bier and N. B Egen, This volume.

APPENDIX

The coefficients of the polynomials are as follows:

$$b_1 = - K_{a1}K_{a2}K_{b1}K_{b2}K_{c1}K_{c2}K_w$$

$$b_2 = - K_{a1}K_{a2}K_{b1}K_{b2}K_{c1}K_{c2}(C_a + C_b + C_c)$$
$$- (K_{a1}K_{a2}K_{b1}K_{b2}K_{c1} + K_{a1}K_{a2}K_{b1}K_{c1}K_{c2} + K_{a1}K_{b1}K_{b2}K_{c1}K_{c2}) K_w$$

$$b_3 = K_{a1}K_{a2}K_{b1}K_{b2}K_{c1}K_{c2}$$
$$- (K_{a1}K_{a2}K_{b1}K_{b2}K_{c1} + K_{a1}K_{a2}K_{b1}K_{c1}K_{c2}) C_a$$
$$- (K_{a1}K_{a2}K_{b1}K_{b2}K_{c1} + K_{a1}K_{b1}K_{b2}K_{c1}K_{c2}) C_b$$
$$- (K_{a1}K_{b1}K_{b2}K_{c1}K_{c2} + K_{a1}K_{a2}K_{b1}K_{c1}K_{c2}) C_c$$
$$- (K_{a1}K_{a2}K_{b1}K_{b2} + K_{a1}K_{a2}K_{b1}K_{c1} + K_{a1}K_{b1}K_{b2}K_{c1} + K_{a1}K_{a2}K_{c1}K_{c2}$$
$$+ K_{a1}K_{b1}K_{c1}K_{c2} + K_{b1}K_{b2}K_{c1}K_{c2}) K_w$$

$$b_4 = K_{a1}K_{a2}K_{b1}K_{b2}K_{c1} + K_{a1}K_{a2}K_{b1}K_{c1}K_{c2} + K_{a1}K_{b1}K_{b2}K_{c1}K_{c2}$$
$$+ (K_{b1}K_{b2}K_{c1}K_{c2} - K_{a1}K_{a2}K_{b1}K_{b2} - K_{a1}K_{a2}K_{c1}K_{c2} - K_{a1}K_{a2}K_{b1}K_{c1}) C_a$$
$$+ (K_{a1}K_{a2}K_{c1}K_{c2} - K_{a1}K_{a2}K_{b1}K_{b2} - K_{b1}K_{b2}K_{c1}K_{c2} - K_{a1}K_{b1}K_{b2}K_{c1}) C_b$$
$$+ (K_{a1}K_{a2}K_{b1}K_{b2} - K_{a1}K_{a2}K_{c1}K_{c2} - K_{b1}K_{b2}K_{c1}K_{c2} - K_{a1}K_{b1}K_{c1}K_{c2}) C_c$$
$$- (K_{a1}K_{a2}K_{b1} + K_{a1}K_{b1}K_{b2} + K_{a1}K_{a2}K_{c1} + K_{a1}K_{b1}K_{c1} + K_{b1}K_{b2}K_{c1}$$
$$+ K_{a1}K_{c1}K_{c2} + K_{b1}K_{c1}K_{c2}) K_w$$

$$b_5 = K_{a1}K_{a2}K_{b1}K_{b2} + K_{a1}K_{a2}K_{b1}K_{c1} + K_{a1}K_{b1}K_{b2}K_{c1} + K_{a1}K_{a2}K_{c1}K_{c2}$$
$$+ K_{a1}K_{b1}K_{c1}K_{c2} + K_{b1}K_{b2}K_{c1}K_{c2}$$
$$+ (K_{b1}K_{b2}K_{c1} + K_{b1}K_{c1}K_{c2} - K_{a1}K_{a2}K_{c1} - K_{a1}K_{a2}K_{b1}) C_a$$
$$+ (K_{a1}K_{a2}K_{c1} + K_{a1}K_{c1}K_{c2} - K_{b1}K_{b2}K_{c1} - K_{a1}K_{b1}K_{b2}) C_b$$
$$+ (K_{a1}K_{a2}K_{b1} + K_{a1}K_{b1}K_{b2} - K_{a1}K_{c1}K_{c2} - K_{b1}K_{c1}K_{c2}) C_c$$
$$+ (K_{a1}K_{a2} + K_{a1}K_{b1} + K_{b1}K_{b2} + K_{a1}K_{c1} + K_{b1}K_{c1} + K_{c1}K_{c2}) K_w$$

$$b_6 = K_{a1}K_{a2}K_{b1} + K_{a1}K_{b1}K_{b2} + K_{a1}K_{a2}K_{c1} + K_{a1}K_{b1}K_{c1} + K_{b1}K_{b2}K_{c1} + K_{a1}K_{c1}K_{c2} + K_{b1}K_{c1}K_{c2}$$

$$+ (K_{b1}K_{b2} + K_{c1}K_{c2} + K_{b1}K_{c1} - K_{a1}K_{a2})\, C_a$$

$$+ (K_{a1}K_{a2} + K_{c1}K_{c2} + K_{a1}K_{c1} - K_{b1}K_{b2})\, C_b$$

$$+ (K_{a1}K_{a2} + K_{b1}K_{b2} + K_{a1}K_{b1} - K_{c1}K_{c2})\, C_c$$

$$- (K_{a1} + K_{b1} + K_{c1})\, K_w$$

$$b_7 = K_{a1}K_{a2} + K_{a1}K_{b1} + K_{b1}K_{b2} + K_{a1}K_{c1} + K_{b1}K_{c1} + K_{c1}K_{c2}$$

$$+ (K_{b1} + K_{c1})\, C_a + (K_{a1} + K_{c1})\, C_b + (K_{a1} + K_{b1})\, C_c$$

$$- K_w$$

$$b_8 = K_{a1} + K_{b1} + K_{c1} + C_a + C_b + C_c$$

Table 1: Assumed Constants*

Component	pK_1	pK_2	$u(10^5)cm^2V^{-1}sec^{-1}$	$D(10^5)cm^2sec^{-1}$
A - Glutamic acid	2.19	4.25	31.7	0.80
B - Histidine	6.00	9.17	32.4	0.73
C - Unspecified component	4.00	6.00	30.0	0.80

* pK Values were taken from reference 11; diffusion coefficient for histidine from reference 12; diffusion coefficient for glutamic acid was calculated from the values of the equivalent conductance[13]; mobilities were taken as an average of the values for the anionic and cationic species.

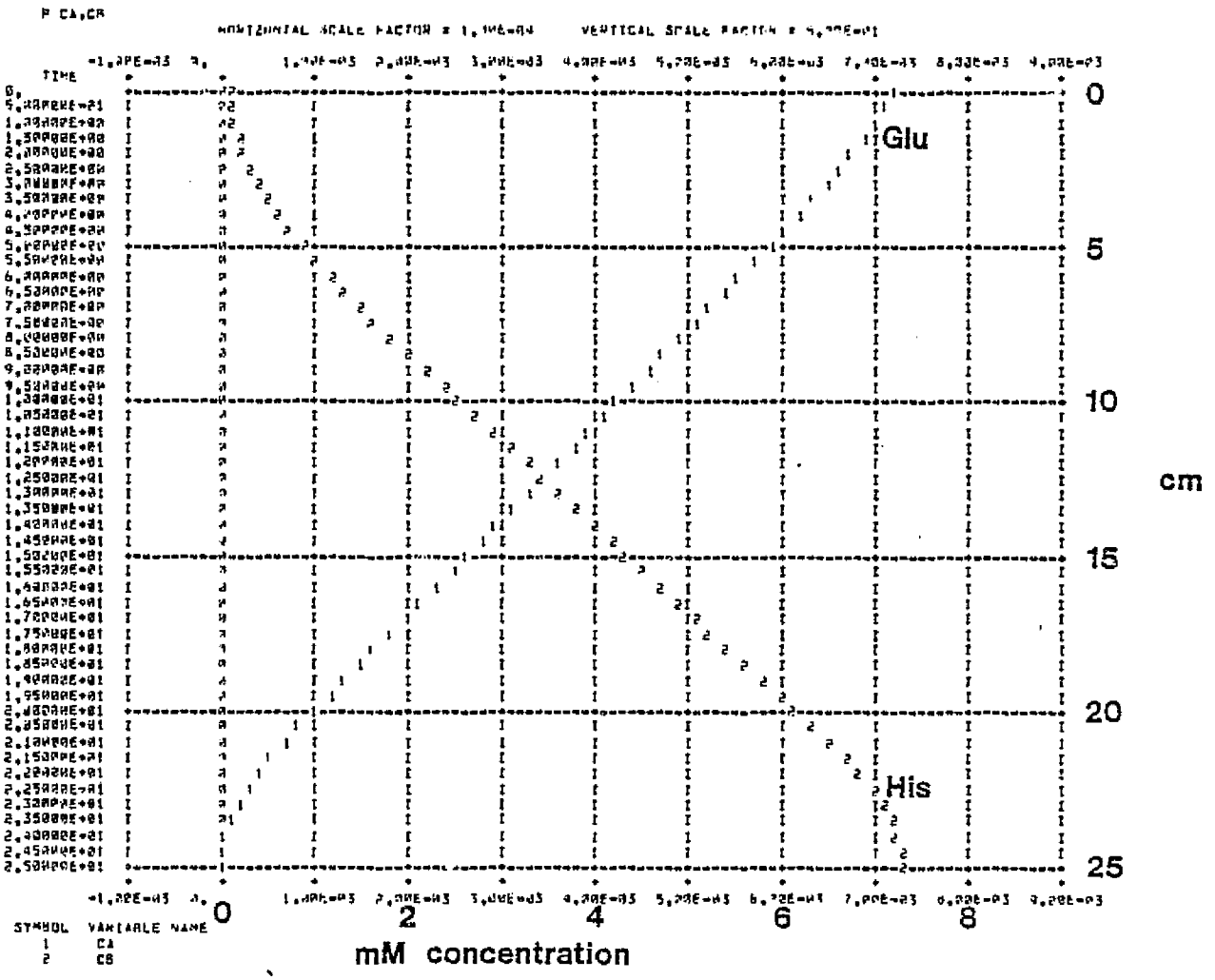

Fig. 1: The concentration profiles of the two-component IEF system using glutamic acid and histidine. The amperage employed was 4×10^{-7}A.

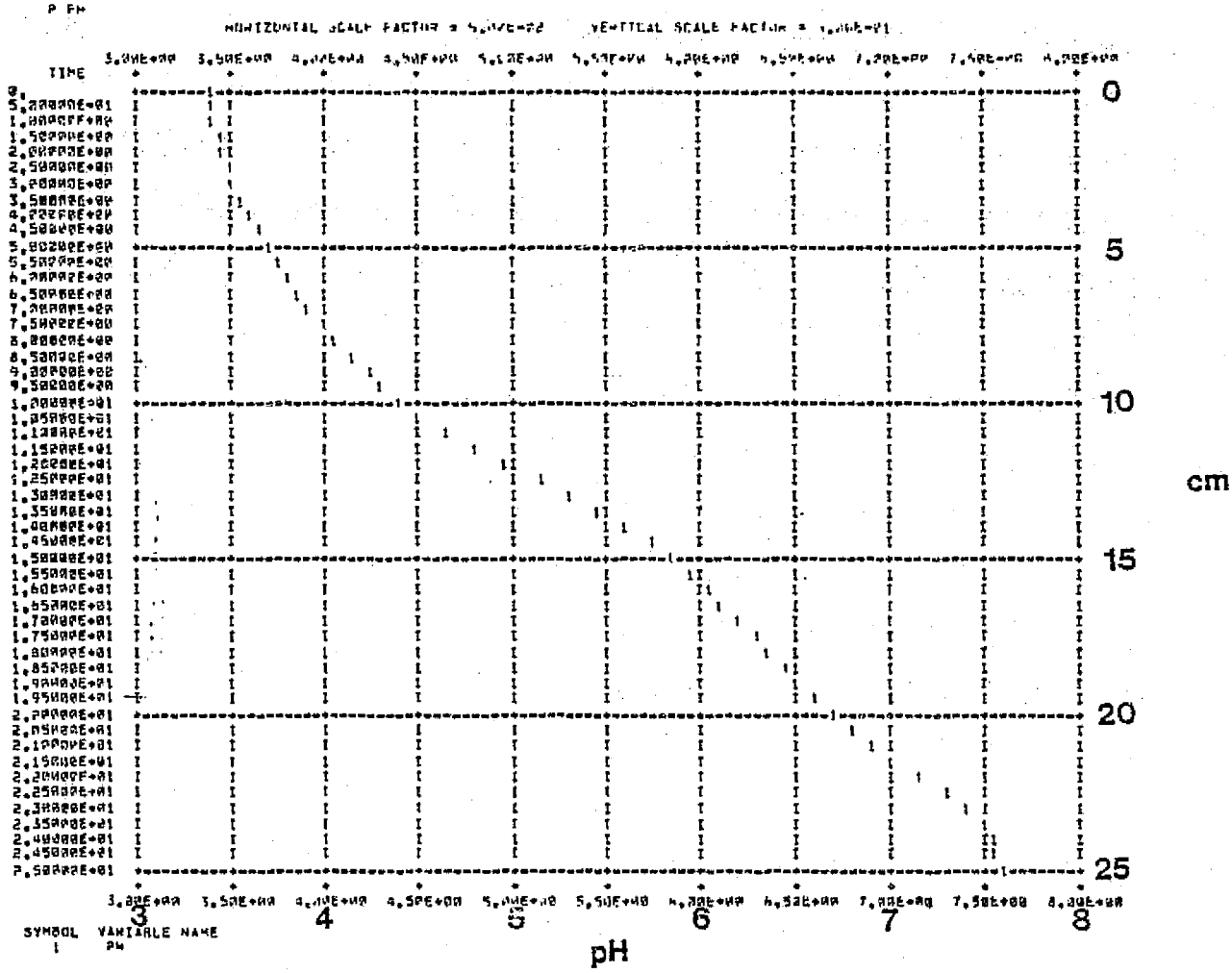

Fig. 2: The pH profile of the two-component system. The conditions were identical to Fig. 1.

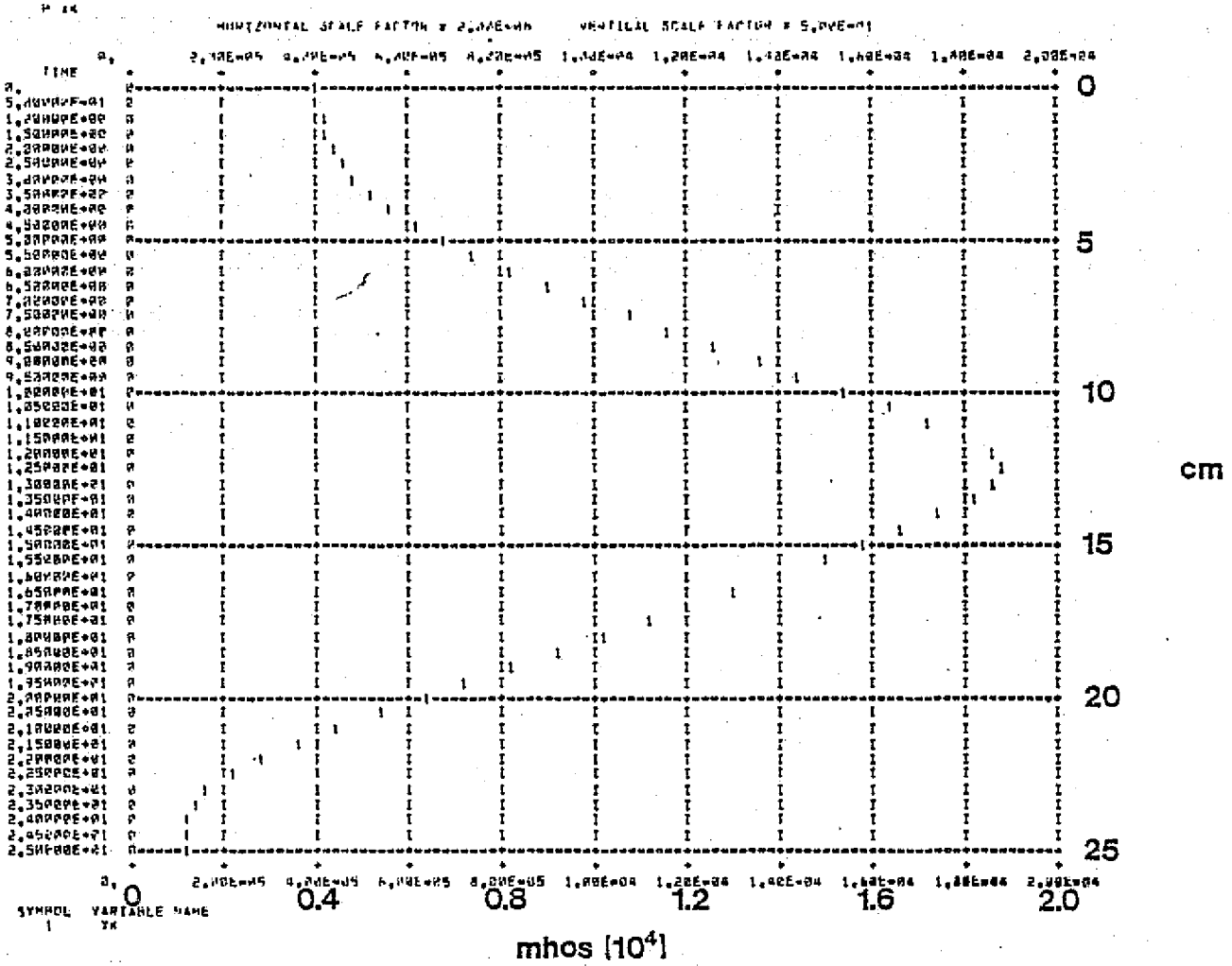

Fig. 3: The conductance profile of the two-component system. The conditions were identical to Fig. 1.

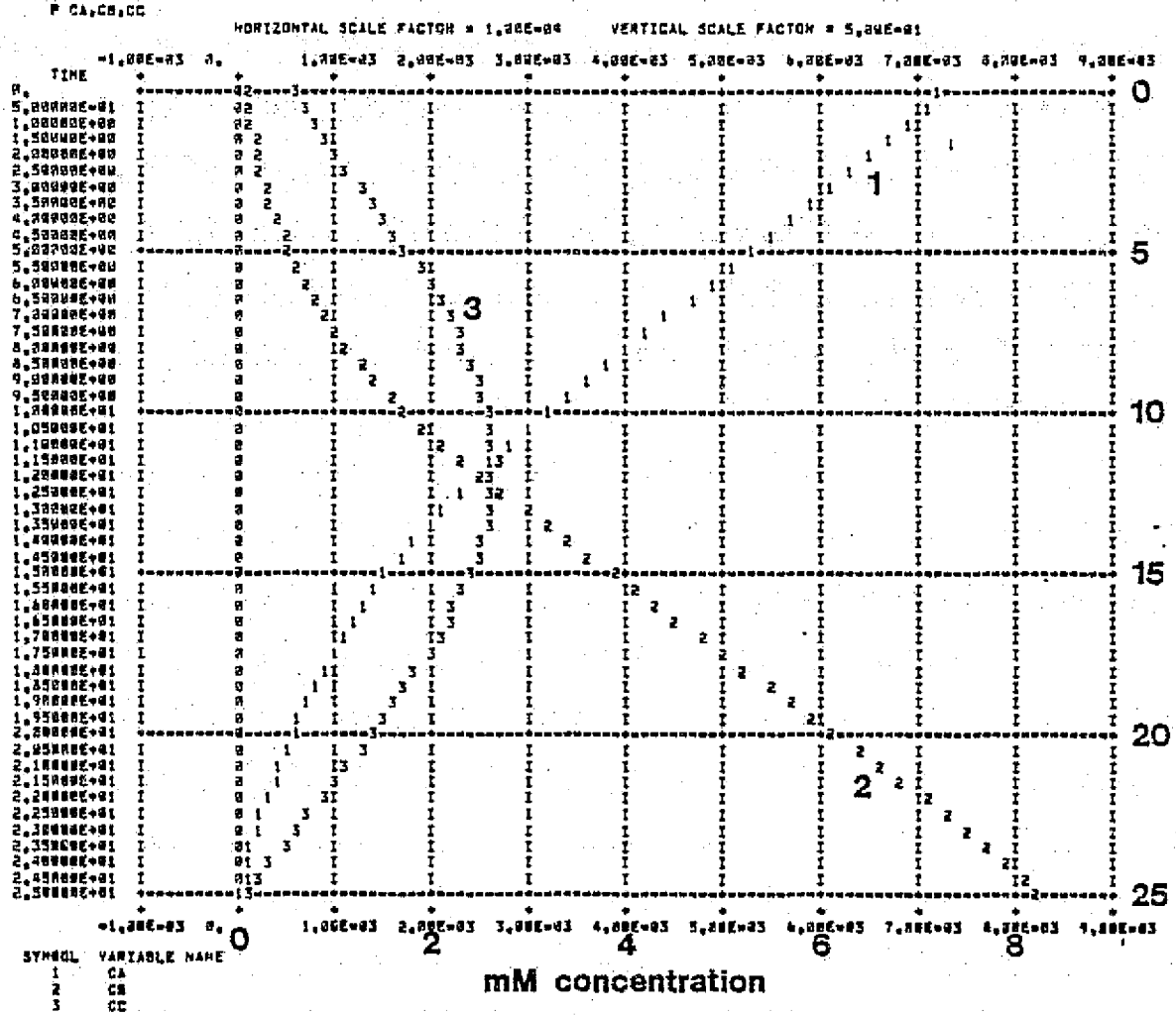

Fig. 4: The concentration profiles of the three-component IEF system. The amperage employed was 5×10^{-7}A.

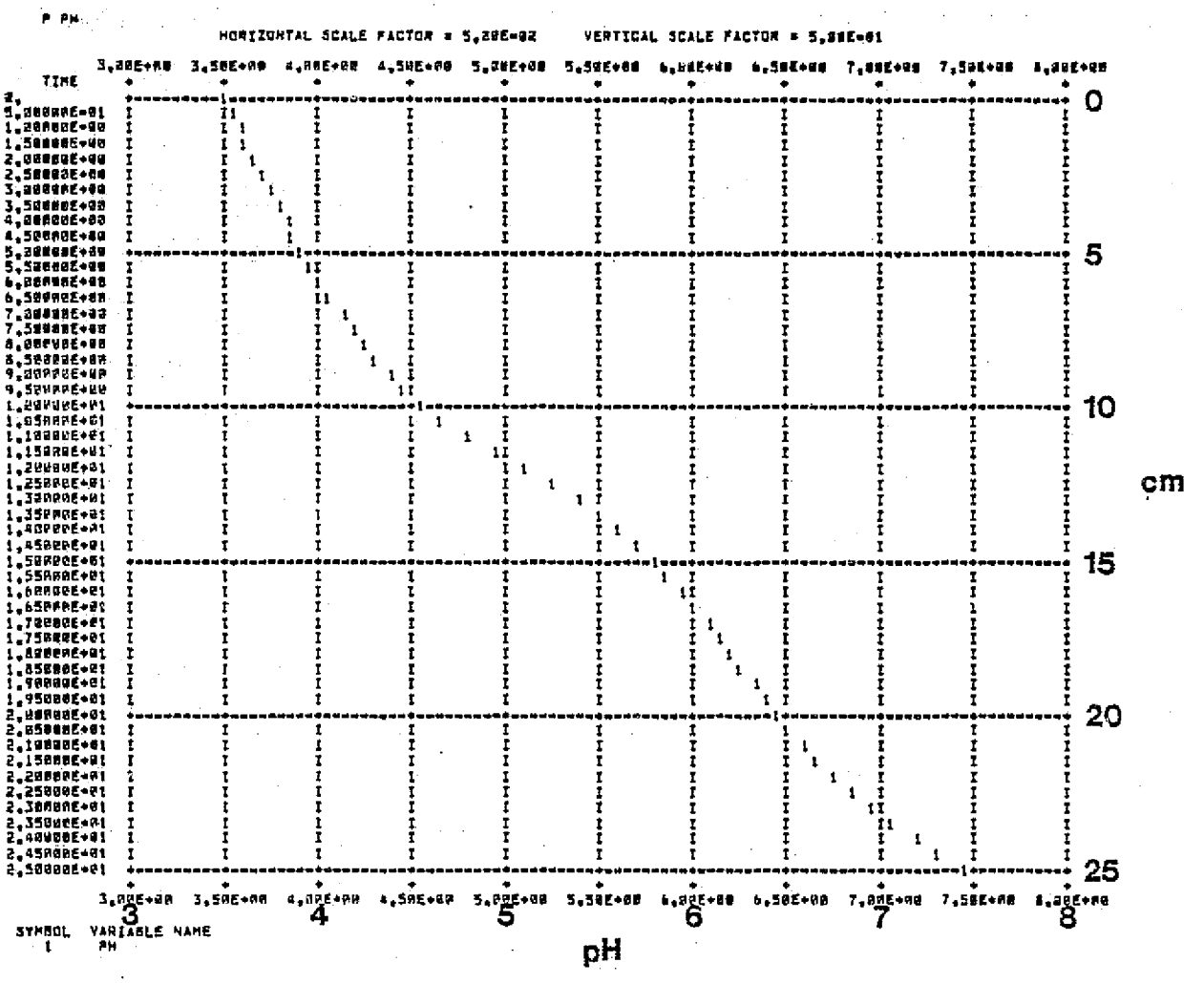

Fig. 5: The pH profile of the three-component system. The conditions were identical to Fig. 4.

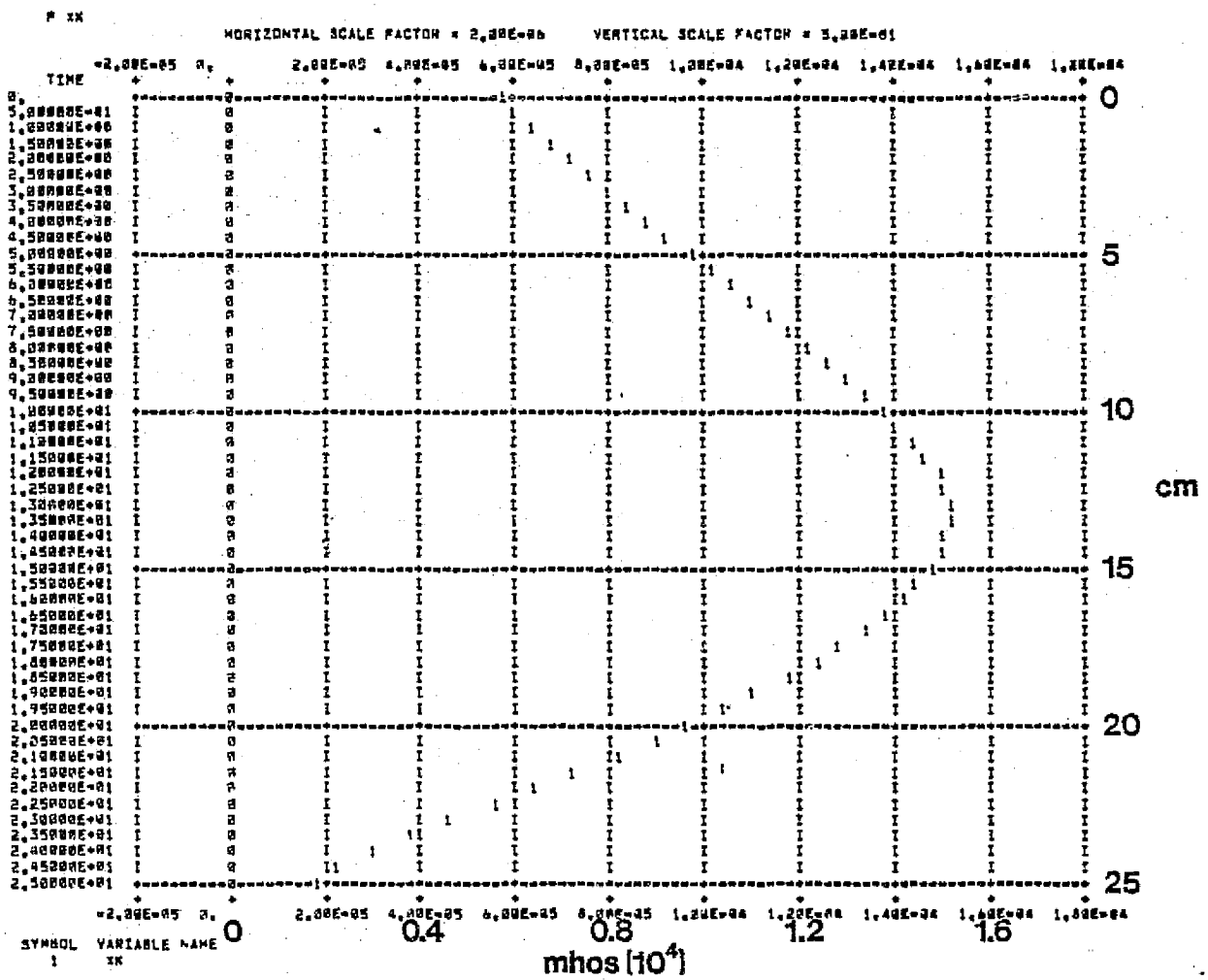

Fig. 6: The conductance profile of the three-component system. The conditions were identical to Fig. 4.

APPENDIX B

MATHEMATICAL MODEL OF STEADY-STATE ISOELECTRIC FOCUSING SYSTEM OF N-COMPONENTS

O. A. PALUSINSKI

Title

Mathematical Model of a Steady-State Isoelectric Focusing System of N-Components

Abstract

The paper presents basic equations expressing the concentrations of cationic and anionic ampholytes in terms of hydrogen ion concentration, corresponding dissociation constants and ampholyte concentrations. Balance between electromigration and diffusion movement determines the set of differential equations. Solution of these equations gives the ampholyte concentration as function of distance x, along the column axis. The differential equations are coupled by the polynomial of order 2N+2, which results from the electroneutrality equation. The coefficients of the polynomial are complicated functions of dissociation constants and ampholtye concentrations. The recurrence formula for these coefficients is derived in the first part of the paper.

Introduction

In an earlier paper ( ) a mathematical model was presented for a three-component isoelectric focusing system. The model provided the means of computing ampholytes' concentrations, the pH, and the conductance at every point along the column axis in terms of the components' mobilities, diffusion coefficients, and proton dissociation constants. The model consists of an ordinary differential equation for each component and a single algebraic coupling equation. The differential equations express the steady-state balance that exists between the mass transports resulting from diffusion and electromigration. The algebraic polynomial is a statement of the condition of electroneutality. The equations of the two and three component models were derived directly from the fundamental relations. In order to conveniently implement the model with higher multiple component systems, the model equations have been generalized and an algorithm has been developed to generate the differential equations and coupling polynomial for an N component system.

Notation

C_i^+ - the concentration of cationic ampholyte (ith comp.)

C_i^- - the concentration of anionic (units

h - hydrogen ion concentration (units)

K_{i1}, K_{i2} - the first dissociation constants of the ampholyte (titrated from isoel. state with acid and base respectively).

u_i - component mobility

q - cross-sectional area

D_i - diffusion coefficient

K_w - ion product of water

1. BASIC EQUATIONS

$$C_i^+ = \frac{h^2 C_i}{h^2 + hK_{i1} + K_{i1}K_{i2}} \qquad (1)$$

$$C_i^- = \frac{K_{i1}K_{i2} C_i}{h^2 + hK_{i1} + K_{i1}K_{i2}} \qquad (2)$$

$$i = 1, 2, \ldots, N$$

CONDUCTANCE

$$K = \frac{F}{1000} \sum_{i=1}^{N} u_i (C_i^+ + C_i^-) \qquad (3)$$

ELECTROMIGRATION

$$Je^i = \frac{I}{qK} u_i (C_i^+ - C_i^-)$$

DIFFUSION

$$Jd^i = - D_i \frac{dC_i}{dx}$$

BALANCE ($Je^i = -Jd^i$)

$$\frac{dC_i}{dx} = \frac{I}{D_i qK} u_i (C_i^+ - C_i^-) \qquad (4)$$

ELECTRONEUTRALITY

$$h + \sum_{i=1}^{N} C_i^+ = K_w/h + \sum_{i=1}^{N} C_i^- \qquad (5)$$

2. DIFFERENTIAL EQUATIONS

(1), (2) → (3)

$$K = \frac{F}{1000} \sum_{i=1}^{N} u_i \frac{h^2 + K_{i1}K_i}{h^2 + hK_{i1} + K_{i1}K_{i2}} C_i \qquad (6)$$

(1), (2) → (4)

$$\frac{dC_i}{dx} = \frac{I}{D_i q K} u_i \frac{h^2 - K_{i1}K_{i2}}{h^2 + hK_{i1} + K_{i1}K_{i2}} C_i \qquad (7)$$

(6) → (7)

$$\frac{dC_i}{dx} = \frac{1000I\ u_i}{F\ D_i\ q} \frac{h^2 - K_{i1}K_{i2}}{h^2 + hK_{i1} + K_{i1}K_{i2}} \frac{1}{Q} C_i \qquad (8)$$

$$Q = \sum_{i=1}^{N} \frac{h^2 + K_{i1}K_{i2}}{h^2 + hK_{i1} + K_{i1}K_{i2}} u_i C_i \qquad (9)$$

3. POLYNOMIAL

(1), (2) → (5)

$$h + \sum_{i=1}^{N} \frac{h^2 C_i}{h^2 + hK_{i1} + K_{i1}K_{i2}} = K_w/h + \sum_{i=1}^{N} \frac{K_{i1}K_{i2} C_i}{h^2 + hK_{i1} + K_{i1}K_{i2}} \qquad (10)$$

$$h^2 + \sum_{i=1}^{N} \frac{h^3 C_i - K_{i1}K_{i2}hC_i}{h^2 + hK_{i1} + K_{i1}K_{i2}} = K_w \Big/ \prod_{j=1}^{N} (h^2 + hK_{j1} + K_{j1}K_{j2}) \qquad (11)$$

$$h^2 \prod_{j=1}^{N} (h^2+hK_{j1}+K_{j1}K_{j2}) + \sum_{i=1}^{N} (h^3C_i-hK_{i1}K_{i2}C_i) \prod_{\substack{j=1 \\ j\neq i}}^{N} (h^2+hK_{j1}+K_{j1}K_{j2}) =$$

$$= K_w \prod_{j=1}^{N} (h^2 + hK_{j1} + K_{j1}K_{j2}) \qquad (12)$$

Notation:

$$\begin{aligned} A_i &= K_{i1} \\ B_i &= K_{i1}K_{i2} \end{aligned} \qquad (13)$$

$$h^2 \prod_{j=i}^{N} (h^2+hA_j+B_j) + \sum_{i=1}^{N} (h^3C_i-hB_iC_i) \prod_{\substack{j=1 \\ j\neq i}}^{N} (h^2 + hA_j + B_j) =$$

$$= K_w \prod_{j=1}^{N} (h^2 + hA_j + B_j) \qquad (14)$$

$$P_N = \prod_{j=1}^{N} (h^2+hA_j+B_j) = (h^2+hA_1+B_1)(h^2+hA_2+B_2)(h^2+hA_3+B_3)....$$

$$....(h^2 + hA_n + B_n)$$

$$P_{N,1} = \prod_{j=2}^{N} (h^2 + hA_j + B_j)$$

$$P_{N,2} = \prod_{\substack{j=1 \\ j\neq 2}}^{N} (h^2 + hA_j + B_j)$$

$$\vdots$$

$$P_{N,i} = \prod_{\substack{j=1 \\ j\neq i}}^{N} (h^2 + hA_j + B_j) \qquad (15)$$

$$\vdots$$

$$P_{N,N-1} = \prod_{\substack{j=1 \\ j\neq N-1}}^{N} (h^2 + hA_j + B_j)$$

$$P_{N,N} = \prod_{j=1}^{N-1} (h^2 + hA_j + B_j)$$

Using the notation (15) we can write (14) in the form

$$h^2 P_N + \sum_{i=1}^{N} (h^3 C_i - hB_i C_i) P_{N,i} = K_w P_N \qquad (16)$$

The (16)is the general form of the polynomial in the case of N- component.

4. THE RECURRENCE RELATIONS FOR THE POLYNOMIAL COEFFICIENTS

4.1 Fundamental relation

The polynomial (16) can be written in the form

$$h^2 P_N + \sum_{i=1}^{N} (h^3 C_i - hB_i C_i) P_{N,i} - K_w P_N = 0 \qquad (17)$$

We shall use the notation

$$\psi_N(h) = h^2 P_N + \sum_{i=1}^{N} (h^3 C_i - hB_i C_i) P_{N,i} - K_w P_N \qquad (18)$$

Expressing P_N and $P_{N,i}$ explicitly in (18), performing suitable operation and grouping the terms with respect to the powers of h we obtain

$$\psi_N(h) = \sum_{i=o}^{2N+2} h^i \, {}^{N}a_i \qquad (19)$$

where ${}^{N}a_i$ - coefficient of the polynomial in case of N-components.

The polynomial for the case of N+1 components has the form

$$h^2 P_{N+1} + \sum_{i=1}^{N+1} (h^3 C_i - h B_i C_i) P_{N+1,i} - K_w P_{N+1} = 0 \qquad (20)$$

derived directly from (17).

The formula (20) can be written in the form

$$h^2 P_{N+1} + \sum_{i=1}^{N} (h^3 C_i - hB C_i) P_{N+1,i} - K_w P_{N+1} + (h^3 C_{N+1} - hB_{N+1} C_{N+1}) P_{N+1,N+1} = 0 \qquad (21)$$

From (15) we obtain

$$P_{N+1} = P_N(h^2 + hA_{N+1} + B_{N+1})$$

$$P_{N+1,i} = P_{N,i}(h^2 + hA_{N+1} + B_{N+1}) \qquad (22)$$

$$\vdots \qquad\qquad i = 1,2,\ldots,N$$

$$P_{N+1,N+1} = P_N$$

Using (22) in (21) we obtain

$$h^2P_N + \sum_{i=1}^{N}(h^3C_i - hB_iC_i)P_{N,i} - K_wP_N\ (h^2 + hA_{N+1} + B_{N+1}) +$$

$$+ (h^3C_{N+1} - h\,B_{N+1}\,C_{N+1}) = 0 \qquad (23)$$

Taking into account notation (23) we obtain the polynomial for N+1 components expressed in terms of polynomial for N components

$$\psi_N(h)(h^2+hA_{N+1} + B_{N+1}) + (h^3C_{N+1} - hB_{N+1}C_{N+1})\ P_N = 0 \qquad (24)$$

The above polynomial for N+1 components can be divided into two parts

$$\Gamma = \psi_N(h)(h^2 + h\,A_{N+1} + B_{N+1}) \qquad (25)$$

$$\Omega = (h^2\,C_{N+1} - h\,B_{N+1}\,C_{N+1})\ P_N \qquad (26)$$

Substituting (19) to (25) we obtain after some manipulations

$$\Gamma = \sum_{i=o}^{2N+4} h^i \left({}^{N}a_{i-2} + {}^{N}a_{i-1} A_{N+1} + {}^{N}a_i B_{N+1} \right) \tag{27}$$

with

$$a_{2N+2} = 1$$

$$a_{-k} = a_{2N+2+k} = 0$$

$$\text{for } k = 1,2,\ldots .$$

In order to determine the coefficients of Ω we have to find the expression for P_N.

4.2 Finding the recurrance relations for P_N.

We shall use the notation

$$P_N = \sum_{j=o}^{2N} h^j \; {}^{N}\alpha_j \qquad ; \quad {}^{N}\alpha_{2N} = 1 \tag{28}$$

From (22) we have

$$P_{N+1} = P_N \left(h^2 + h A_{N+1} + B_{N+1} \right) \tag{29}$$

Substituting (28) to (29) we obtain after some manipulations

$$P_{N+1} = \sum_{j=o}^{2N+2} h^j \left({}^{N}\alpha_{j-2} + {}^{N}\alpha_{j-1} A_{N+1} + {}^{N}\alpha_j B_{N+1} \right) \tag{30}$$

where

$${}^{N}\alpha_{-k} = {}^{N}\alpha_{2N+k} = 0$$

$$\text{for } k = 1,2.$$

The formula (30) permits computing the coefficients of P_{N+1} based on the coefficients of P_N

$$ {}^{N+1}\alpha_j = {}^{N}\alpha_{j-2} + {}^{N}\alpha_{j-1}\ A_{N+1} + {}^{N}\alpha_j\ B_{N+1} \tag{31} $$

this way we can successively compute P_2, P_3, ..., etc.

Substituting (28) to (26) yields after some manipulations

$$ \Omega = \sum_{i=o}^{2N+4} h^i\ ({}^{N}\alpha_{i-3} - {}^{N}\alpha_{i-1}\ B_{N+1})\ C_{N+1} \tag{32} $$

$$ {}^{N}\alpha_{-k} = {}^{N}\alpha_{2N+k} = 0 \text{ for } k = 1,2,3 $$

$$ {}^{N}\alpha_{2N} = 1 $$

4.3 Recurrence notation for the polynomial coefficients.

The polynomial for N+1 components given by formula (24) can be written in the form

$$ \psi_{N+1}(h) = \Gamma + \Omega \tag{33} $$

where Γ and Ω are specified by (25),(26) or (27),(32).

Substituting (27) and (32) to (33) yields

$$ \psi_{N+1}(h) = \sum_{i=o}^{2N+4} h^i \left[{}^{N}a_{i-2} + {}^{N}a_{i-1}\ A_{N+1} + {}^{N}a_i B_{N+1} + ({}^{N}\alpha_{i-3} - {}^{N}\alpha_{i-1} B_{N+1}) C_{N+1} \right] \tag{34} $$

From (34) we obtain the recurrence formula for the coefficients of the polynomial in the form

$$ {}^{N+1}a_l = {}^{N}a_{i-2} + {}^{N}a_{i-1} A_{N+1} + {}^{N}a_i B_{N+1} + ({}^{N}\alpha_{i-3} - {}^{N}\alpha_{i-1} B_{N+1}) C_{N+1} \qquad (35) $$

$$ i = 0,1,2,\ldots, 2N+4 $$

$$ {}^{N}a_{-k} = {}^{N}a_{2N+2+k} = 0 $$

$$ {}^{N}\alpha_{-k} = {}^{N}\alpha_{2N+k} = 0 $$

$$ k = 1,2,3 $$

APPENDIX C

INDEX OF LIBRARY OF COMPUTER SIMULATIONS

Identification		Dissociation Constants							Concentrations			Mobilities			Diffusion Constant		
No.	Date Time	A1	A-2	B-1	B-2	C-1	C-2	Crt.	A	B	C	A	B	C	A	B	C
1.	4/7 14:37	2.19	4.25	6.0	9.17			1x-5	3.4x-3	3.4x-3		30.0x-5	30.0x-5		0.9x-5	0.9x-5	
2.	4/7 14:03	2.19	4.25	6.0	9.17			1x-5	2.78-5	2.78x-5		30.0x-5	30.0x-5		0.9x-5	0.9x-5	
3.	4/12 9:39	2.19	4.25	6.0	9.17			1x-6	7.2x-3	8.1x-5		31.7x-5	32.4x-5		0.8x-5	0.73x-5	
4.	4/12 9:48	2.19	4.25	6.0	9.17			1x-7	7.2x-3	8.1x-5		31.7x-5	32.4x-5		0.8x-5	0.73x-5	
5.	4/12 10:10	2.19	4.25	6.0	9.17			4x-7	7.2x-3	8.1x-5		31.7x-5	32.4x-5		0.8x-5	0.73x-5	
6.	4/12 12:21	2.19	4.25	6.0	9.17			2x-7	7.2z-3	8.1x-5		31.7x-5	32.4x-5		0.8x-5	0.8x-5	
7.	4/12 9:53	2.19	4.25	6.0	9.17			5x-7	7.24x-3	8.1x-5		31.7x-5	32.4x-5		0.8x-5	0.73x-5	
8.	4/12 12:33	2.19	4.25	6.10	9.17			2x-7	5.46x-3	1.23x-3		31.7x-5	32.4x-5		0.8x-5	0.73x-5	
9.	4/12 12:39	2.19	4.25	6.0	9.17			5x-7	7.69x-8	7.27x-3		31.7x-5	32.4x-5		0.8x-5	0.73x-5	
10.	4/12 12:43	2.19	4.25	6.0	9.17			4x-7	7.24x-3	8.1x-5		31.7x-5	32.4x-5		0.8x-5	0.73x-5	
11.	4/12 12:26	2.19	4.25	6.0	9.17			4x-7	7.24x-3	8.1x-5		31.7x-5	32.4x-5		0.8x-5	0.73x-5	
12.	4/24 21:23	2.19	4.25	6.0	9.17			4x-7	7.24x-3	8.1x-5		31.7x-5	32.4x-5		0.8x-5	0.73x-5	
13.	4/28 16:44	2.19	4.25	6.0	9.17			4x-7	7.24x-3	8.1x-5		31.7x-5	32.4x-5		0.8x-5	0.73x-5	
14.	5/2 16:16	0.19	6.25	4.11.17				4x-7	7.24x-3	8.1x-5		31.7x-5	32.4x-5		0.8x-5	0.73x-5	
15.	5/2 17:00	0.19	6.25	4.0	11:17			4x-7	7.24x-3	8.1x-5		31.7x-5	32.4x-5		0.8x-5	0.73x-5	
16.	4/29 21:16	2.19	4.25	6.0	9.17	4.0	6.0	4x-6	7.24x-3	8.1x-5	6.0x-4	31.7x-5	32.4x-5	30.0x-5	0.8x-5	0.73x-5	0.8x-5
17.	4/30 12:16	2.19	4.25	6.0	9.17	4.0	6.0	4x-6	7.24x-3	8.1x-5	6.0x-4	31.7x-5	32.4x-5	30.0x-5	0.8x-5	0.73x-5	0.8x-5
18.	4/30 12:18	2.19	4.25	6.0	9.17	4.0	6.0	4x-6	7.24x-3	8.1x-5	6.0x-4	31.7x-3	32.4x-5	30.0x-5	0.8x-5	0.73x-5	0.8x-5
19.	4/30 12:37	2.19	4.25	6.0	9.17	4.0	6.0	4x-7	7.24x-3	8.1x-5	6.0x-4	31.7x-5	32.4x-5	30.0x-5	0.8x-5	0.73x-5	0.8x-5
20.	5/2 16:48	2.19	4.25	6.0	9.17	4.0	6.0	6x-7	7.24x-3	8.1x-5	6.0x-4	31.7x-5	32.4x-5	30.0x-5	0.8x-5	0.73x-5	0.8x-5
21.	5/2 16:55	2.19	4.25	6.0	9.17	4.0	6.0	5x-7	7.24x-3	8.1x-5	6.0x-4	31.7x-5	32.4x-5	30.0x-5	0.8x-5	0.73x-5	0.8x-5

Identification			Dissociation Constants							Concentrations			Mobilities			Diffusion Constant		
No.	Date	Time	A1	A-2	B-1	B-2	C-1	C-2	Crt.	A	B	C	A	B	C	A	B	C
1.	6/15	13:22	2.0	4.0	6.0	8.0			4x-7	7.24x-3	8.1x-5		30.0x-5	30.0x-5		0.8x-5	0.8x-5	
2.	6/15	13:23	2.0	4.0	6.0	8.0			4x-7	7.24x-3	8.1x-5		30.0x-5	30.0x-5		0.8x-5	0.8x-5	
3.	6/15	13:24	2.0	4.0	5.0	9.0			4x-7	7.24x-3	8.1x-5		30.0x-5	30.0x-5		0.8x-5	0.8x-5	
4.	6/15	13:28	2.0	4.0	5.0	9.0			4x-7	7.24x-3	8.1x-5		30.0x-5	30.0x-5		0.8x-5	0.8x-5	
5.	6/15	13:42	1.0	5.0	6.0	8.0			4x-7	7.24x-3	8.1x-5		30.0x-5	30.0x-5		0.8x-5	0.8x-5	
6.	6/15	13:32	2.0	4.0	4.0	10.0			4x-7	7.24x-3	8.1x-5		30.0x-5	30.0x-5		0.8x-5	0.8x-5	
7.	6/15	13:43	3.0	5.0	6.0	8.0			4x-7	7.24x-3	8.1x-5		30.0x-5	30.0x-5		0.8x-5	0.8x-5	
8.	6/15	13:45	4.0	6.0	6.0	8.0			4x-7	7.24x-3	8.1x-5		30.0x-5	30.0x-5		0.8x-5	0.8x-5	
9.	6/16	9:47	5.0	7.0	6.0	8.0			4x-7	7.24x-3	8.1x-5		30.0x-5	30.0x-5		0.8x-5	0.8x-5	
10.	6/16	9:50	5.5	7.5	6.0	8.0			4x-7	7.24x-3	8.1x-5		30.0x-5	30.0x-5		0.8x-5	0.8x-5	
11.	6/16	9:51	2.0	4.0	6.0	8.0			4x-7	7.24x-3	8.1x-5		30.0x-5	30.0x-5		0.8x-5	0.8x-5	
12.	6/16	9:59	1.0	9.0	6.0	8.0			4x-7	3.0x-3	3.0x-3		30.0x-5	30.0x-5		0.8x-5	0.8x-5	
13.	6/16	10:00	2.0	8.0	6.0	8.0			4x-7	3.0x-3	3.0x-3		30.0x-5	30.0x-5		0.8x-5	0.8x-5	
14.	6/16	9:57	3.0	7.0	6.0	8.0			4x-7	3.0x-3	3.0x-3		30.0x-5	30.0x-5		0.8x-5	0.8x-5	
15.	6/16	9:56	4.0	6.0	6.0	8.0			4x-7	3.0x-3	3.0x-3		30.0x-5	30.0x-5		0.8x-5	0.8x-5	
16.	6/16	9:53	2.0	4.0	6.0	8.0			4x-7	3.0x-3	3.0x-3		30.0x-5	30.0x-5		0.8x-5	0.8x-5	
17.	6/30	8:49	5.5	7.5	6.0	8.0			2x-6	3.0x-3	3.0x-3		30.0x-5	30.0x-5		0.8x-5	0.8x-5	
18.	6/30	8:44	1.0	9.0	6.0	8.0			4x-6	1.5x-2	1.5x-2		30.0x-5	30.0x-5		0.8x-5	0.8x-5	
19.	6/29	16:55	5.0	7.0	6.0	8.0			4x-6	3.0x-3	3.0x-3		30.0x-5	30.0x-5		0.8x-5	0.8x-5	
20.	6/30	8:52	5.5	7.5	6.0	8.0			4x-6	3.0x-3	3.0x-3		30.0x-5	30.0x-5		0.8x-5	0.8x-5	
21.	6/29	15:43	1.0	9.0	6.0	8.0			4x-6	3.0x-3	3.0x-3		30.0x-5	30.0x-5		0.8x-5	0.8x-5	
22.	6/30	8:25	1.0	9.0	6.0	8.0			4x-6	3.0x-2	3.0x-2		30.0x-5	30.0x-5		0.8x-5	0.8x-5	
23.	6/29	16:53	5.0	7.0	6.0	8.0			2x-6	3.0x-3	3.0x-3		30.0x-5	30.0x-5		0.8x-5	0.8x-5	
24.	6/30	8:22	1.0	9.0	6.0	8.0			4x-6	3.0x-2	3.0x-2		30.0x-5	30.0x-5		0.8x-5	0.8x-5	
25.	6/29	17:06	1.0	9.0	6.0	8.0			4x-7	3.0x-3	3.0x-3		30.0x-5	30.0x-5		0.8x-5	0.8x-5	

Identification		Dissociation Constants							Concentrations			Mobilities			Diffusion Constant		
No.	Date Time	A1	A-2	B-1	B-2	C-1	C-2	Crt.	A	B	C	A	B	C	A	B	C
26.	6/29 17:04	2.0	8.0	6.0	8.0			4x-7	3.0x-3	3.0x-3		30.0x-5	30.0x-5		0.8x-5	0.8x-5	
27.	6/29 16:58	5.5	7.5	6.0	8.0			4x-6	3.0x-3	3.0x-3		30.0x-5	30.0x-5		0.8x-5	0.8x-5	
28.	6/29 17:02	5.5	7.5	6.0	8.0			2x-6	3.0x-3	3.0x-3		30.0x-5	30.0x-5		0.8x-5	0.8x-5	
29.	6/30 8:47	5.0	7.0	6.0	8.0			2x-6	3.0x-3	3.0x-3		30.0x-5	30.0x-5		0.8x-5	0.8x-5	
30.	6/30 8:45	5.0	7.0	6.0	8.0			4x-6	3.0x-3	3.0x-3		30.0x-5	30.0x-5		0.8x-5	0.8x-5	
31.	6/29 16:51	1.0	9.0	6.0	8.0			4x-6	3.0x-2	3.0x-2		30.0x-5	30.0x-5		0.8x-5	0.8x-5	
32.	6/29 16:49	1.0	9.0	6.0	8.0			4x-6	1.5x-2	1.5x-2		30.0x-5	30.0x-5		0.8x-5	0.8x-5	
33.	6/16 10:19	1.0	9.0	6.0	8.0			4x-7	3.0x-3	3.0x-3		30.0x-5	30.0x-5		0.8x-5	0.8x-5	
34.	6/29 15:41	1.0	9.0	6.0	8.0			2x-6	3.0x-3	3.0x-3		30.0x-5	30.0x-5		0.8x-5	0.8x-5	
35.	6/29 15:48	2.0	8.0	6.0	8.0			4x-6	3.0x-2	3.0x-2		30.0x-5	30.0x-5		0.8x-5	0.8x-5	
36.	6/29 15:46	2.0	8.0	6.0	8.0			4x-6	1.5x-2	1.5x-2		30.0x-5	30.0x-5		0.8x-5	0.8x-5	
37.	6/29 15:38	2.0	8.0	6.0	8.0			4x-6	3.0x-3	3.0x-3		30.0x-5	30.0x-5		0.8x-5	0.8x-5	
38.	6/29 15:35	2.0	8.0	6.0	8.0			2x-6	3.0x-3	3.0x-3		30.0x-5	30.0x-5		0.8x-5	0.8x-5	
39.	7/11 10:57	5.0	7.0	3.0	11.0	7.0	9.0	1x-6	3.0x-3	9.0x-3	3.0x-3	31.7x-5	32.4x-5	30.0x-5	0.8x-5	0.73x-5	0.8x-5
40.	7/11 11:05	5.0	7.0	3.0	11.0	7.0	9.0	2x-7	3.0x-3	9.0x-3	3.0x-3	31.7x-5	32.4x-5	30.0x-5	0.8x-5	0.73x-5	0.8x-5
41.	7/11 10:50	5.0	7.0	3.0	11.0	7.0	9.0	1x-6	3.0x-3	6.0x-3	3.0x-3	31.7x-5	32.4x-5	30.0x-5	0.8x-5	0.73x-5	0.8x-5
42.	7/11 11:07	5.0	7.0	3.0	11.0	7.0	9.0	2x-7	3.0x-3	6.0x-3	3.0x-3	31.7x-5	32.4x-5	30.0x-5	0.8x-5	0.73x-5	0.8x-5
43.	7/11 10:40	5.0	7.0	6.0	8.0	7.0	9.0	1x-6	3.0x-3	12.0x-3	3.0x-3	31.7x-5	32.4x-5	30.0x-5	0.8x-5	0.73x-5	0.8x-5
44.	7/11 10:42	5.0	7.0	6.0	8.0	7.0	9.0	1x-6	3.0x-3	9.0x-3	3.0x-3	31.7x-5	32.4x-5	30.0x-5	0.8x-5	0.73x-5	0.8x-5
45.	7/11 10:31	5.0	7.0	6.0	8.0	7.0	9.0	1x-6	3.0x-3	6.0x-3	3.0x-3	31.7x-5	32.4x-5	30.0x-5	0.8x-5	0.73x-5	0.8x-5
46.	7/11 9:27	2.0	8.0	3.0	9.0			4x-5	6.0x-3	6.0x-3		30.0x-5	30.0x-5		0.8x-5	0.8x-5	
47.	7/11 9:25	2.0	8.0	3.0	9.0			4x-6	6.0x-3	6.0x-3		30.0x-5	30.0x-5		0.8x-5	0.8x-5	
48.	7/11 9:47	2.0	8.0	4.0	10.0			4x-5	6.0x-3	6.0x-3		30.0x-5	30.0x-5		0.8x-5	0.8x-5	
49.	7/11	2.0	8.0	4.0	10.0			4x-6	6.0x-3	6.0x-3		30.0x-5	30.0x-5		0.8x-5	0.8x-5	
50.	7/11 9:13	2.0	8.0	4.0	10.0			4x-6	6.0x-3	6.0x-3		30.0x-5	30.0x-5		0.8x-5	0.8x-5	

Identification		Dissociation Constants							Concentrations			Mobilities			Diffusion Constant		
No.	Date Time	A1	A-2	B-1	B-2	C-1	C-2	Crt.	A	B	C	A	B	C	A	B	C
51.	7/11 10:05	2.0	8.0	4.0	10.0			1x-6	6.0x-3	6.0x-3		30.0x-5	30.0x-5		0.8x-5	0.8x-5	
52.	7/11 10:20	2.0	8.0	4.0	10.0			4x-7	6.0x-3	6.0x-3		30.0x-5	30.0x-5		0.8x-5	0.8x-5	
53.	7/11 9:05	1.0	3.0	2.0	4.0			4x-7	3.0x-3	3.0x-3		30.0x-5	30.0x-5		0.8x-5	0.8x-5	
54.	7/11 9:03	5.0	7.0	6.0	8.0			4x-7	3.0x-3	3.0x-3		30.0x-5	30.0x-5		0.8x-5	0.8x-5	
55.	7/12 15:41	5.0	7.0	6.0	8.0	7.0	9.0	1x-6	2.0x-6	3.0x-3	2.0x-6	30.0x-5	30.0x-5	30.0x-5	0.8x-5	0.8x-5	0.8x-5
56.	7/12 15:46	5.0	7.0	6.4	6.6	6.0	8.0	4x-7	3.0x-3	4.0x-3	3.0x-3	30.0x-5	30.0x-5	30.0x-5	0.8x-5	0.8x-5	0.8x-5
57.	7/13 11:43	5.0	7.0	6.0	8.0	7.0	9.0	1x-6	3.0x-3	2.0x-7	4.0x-18	30.0x-5	30.0x-5	30.0x-5	0.8x-5	0.8x-5	0.8x-5

Identification			Dissociation Constants							Concentrations			Mobilities			Diffusion Constant		
No.	Date	Time	A1	A-2	B-1	B-2	C-1	C-2	Crt.	A	B	C	A	D	C	A	B	C
1.	8/2	21:40	2.19	4.25	4.0	6.0	6.0	9.17	8x-7	8.0x-3	8.0x-5	1.0x-18	31.7x-5	30.0x-5	32.4x-5	0.8x-5	0.8x-5	0.73x-5
2.	8/3	21:29	2.19	4.25	4.0	6.0	6.0	9.17	2x-6	8.0x-3	1.0x-4	1.0x-14	31.7x-5	30.0x-5	32.4x-5	0.8x-5	0.8x-5	0.73x-5
3.	8/4	11:55	4.0	6.0	6.0	8.0	8.0	10.0	2.2x-6	8.0x-3	1.0x-4	1.0x-26	31.7x-5	30.0x-5	32.4x-5	0.8x-5	0.8x-5	0.73x-5
4.	8/3	9:07	2.19	4.25	4.0	6.0	6.0	9.17	1x-6	8.0x-3	8.0x-5	1.0x-11	31.7x-5	30.0x-5	32.4x-5	0.8x-5	0.8x-5	0.73x-5
5.	No Date		2.19	4.25	4.0	6.0	6.0	9.17	1x-6	8.0x-3	1.x-4	1.0x-11	31.7x-5	30.0x-5	32.4x-5	0.8x-5	0.8x-5	0.73x-5
6.	8/4	9:24	2.19	4.25	4.0	6.0	6.0	9.17	2x-6	8.0x-3	1.0x-4	1.0x-18	31.7x-5	30.0x-5	32.4x-5	0.8x-5	0.8x-5	0.73x-5
7.	8/4	9:30	2.19	4.25	4.0	6.0	6.0	9.17	2x-6	8.0x-3	1.0x-4	1.0x-26	31.7x-5	30.0x-5	32.4x-5	0.8x-5	0.8x-5	0.73x-5
8.	8/4	9:43	2.19	4.25	4.0	6.0	6.0	9.17	1.6x-6	8.0x-3	1.0x-4	1.0x-26	31.7x-5	30.0x-5	32.4x-5	0.8x-5	0.8x-5	0.73x-5
9.	8/4	10:31	2.19	4.25	4.0	6.0	6.0	9.17	1.7x-6	8.0x-3	1.0x-4	1.0x-26	31.7x-5	30.0x-5	32.4x-5	0.8x-5	0.8x-5	0.73x-5
10.	8/4	10:40	2.0	4.0	4.0	6.0	6.0	8.0	1.7x-6	8.0x-3	1.0x-4	1.0x-26	31.7x-5	30.0x-5	32.4x-5	0.8x-5	0.8x-5	0.73x-5
11.	8/4	11:06	2.0	4.0	4.0	6.0	6.0	8.0	1.7x-6	8.0x-3	1.0x-4	1.0x-26	30.0x-5	30.0x-5	30.0x-5	0.8x-5	0.8x-5	0.8x-5
12.	8/4	11:20	4.0	6.0	6.0	8.0	8.0	10.0	1.7x-6	8.0x-3	1.0x-4	1.0x-26	31.7x-5	30.0x-5	32.4x-5	0.8x-5	0.8x-5	0.73x-5
13.	8/4	11:34	4.0	6.0	6.0	8.0	8.0	10.0	1.8x-6	8.0x-3	1.0x-4	1.0x-26	31.7x-5	30.0x-5	32.4x-5	0.8x-5	0.8x-5	0.73x-5
14.	8/4	11:40	4.0	6.0	6.0	8.0	8.0	10.0	1.9x-6	8.0x-3	1.0x-4	1.0x-26	31.7x-5	30.0x-5	32.4x-5	0.8x-5	0.8x-5	0.73x-5
15.	8/4	11:46	4.0	6.0	6.0	8.0	8.0	10.0	2.5x-6	8.0x-3	1.0x-4	1.0x-26	31.7x-5	30.0x-5	32.4x-5	0.8x-5	0.8x-5	0.73x-5